Ab initio molecular dynamics calculations on scattering of hyperthermal H atoms from Cu(111) and Au(111)

Geert-Jan Kroes, Michele Pavanello, María Blanco-Rey, Maite Alducin, and Daniel J. Auerbach

Citation: The Journal of Chemical Physics **141**, 054705 (2014); doi: 10.1063/1.4891483
View online: http://dx.doi.org/10.1063/1.4891483
View Table of Contents: http://scitation.aip.org/content/aip/journal/jcp/141/5?ver=pdfcov
Published by the AIP Publishing

Articles you may be interested in

H(D) D(H) + Cu(111) collision system: Molecular dynamics study of surface temperature effects
J. Chem. Phys. **134**, 164306 (2011); 10.1063/1.3583811

In-plane structure and ordering at liquid sodium surfaces and interfaces from ab initio molecular dynamics
J. Chem. Phys. **127**, 134703 (2007); 10.1063/1.2781388

Publisher's Note: "Ab initio molecular dynamics simulation of the H/InP(100)–water interface" [J. Chem. Phys. 117, 872 (2002)]
J. Chem. Phys. **117**, 7816 (2002); 10.1063/1.1503302

Ab initio molecular dynamics simulation of the H/InP(100)–water interface
J. Chem. Phys. **117**, 872 (2002); 10.1063/1.1483070

Ab initio molecular dynamics simulation of the Cu(110)–water interface
J. Chem. Phys. **114**, 3248 (2001); 10.1063/1.1342859

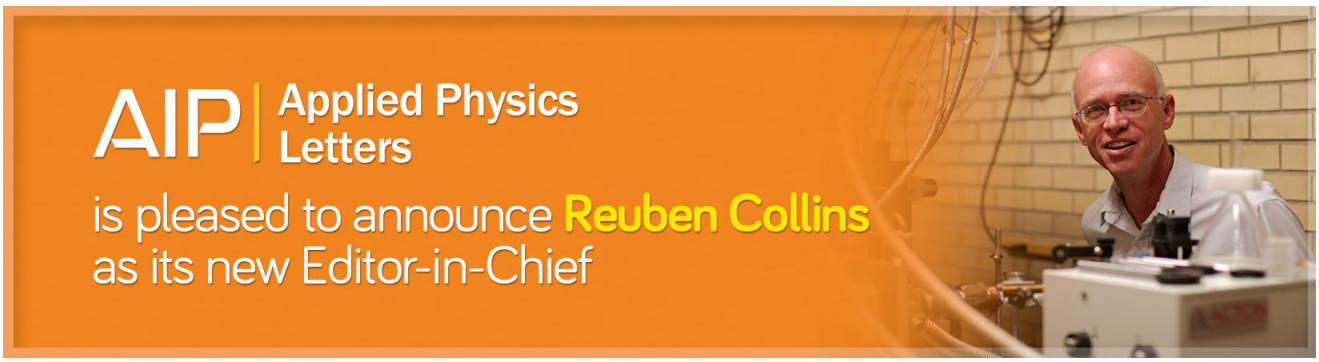

This article is copyrighted as indicated in the article. Reuse of AIP content is subject to the terms at: http://scitation.aip.org/termsconditions. Downloaded to IP: 134.76.223.157 On: Thu, 18 Sep 2014 11:16:10

Ab initio molecular dynamics calculations on scattering of hyperthermal H atoms from Cu(111) and Au(111)

Geert-Jan Kroes,[1,a)] Michele Pavanello,[1,b)] María Blanco-Rey,[2,3] Maite Alducin,[3,4] and Daniel J. Auerbach[1,5,6]

[1]*Leiden Institute of Chemistry, Gorlaeus Laboratories, Leiden University, P.O. Box 9502, 2300 RA Leiden, The Netherlands*
[2]*Departamento de Física de Materiales, Facultad de Químicas UPV/EHU, Apartado 1072, 20080 Donostia-San Sebastián, Spain*
[3]*Donostia International Physics Center, Paseo Manuel de Lardizabal 4, 20018 Donostia-San Sebastián, Spain*
[4]*Centro de Física de Materiales, Centro Mixto CSIC-UPV/EHU, Paseo Manuel de Lardizabal 5, 20018 Donostia-San Sebastián, Spain*
[5]*Max Planck Institute for Biophysical Chemistry, Göttingen, Germany*
[6]*Institute for Physical Chemistry, Georg-August University of Göttingen, Göttingen, Germany*

(Received 13 May 2014; accepted 16 July 2014; published online 4 August 2014)

Energy loss from the translational motion of an atom or molecule impinging on a metal surface to the surface may determine whether the incident particle can trap on the surface, and whether it has enough energy left to react with another molecule present at the surface. Although this is relevant to heterogeneous catalysis, the relative extent to which energy loss of hot atoms takes place to phonons or electron-hole pair (ehp) excitation, and its dependence on the system's parameters, remain largely unknown. We address these questions for two systems that present an extreme case of the mass ratio of the incident atom to the surface atom, i.e., H + Cu(111) and H + Au(111), by presenting adiabatic *ab initio* molecular dynamics (AIMD) predictions of the energy loss and angular distributions for an incidence energy of 5 eV. The results are compared to the results of AIMDEFp calculations modeling energy loss to ehp excitation using an electronic friction ("EF") model applied to the AIMD trajectories, so that the energy loss to the electrons is calculated "post" ("p") the computation of the AIMD trajectory. The AIMD calculations predict average energy losses of 0.38 eV for Cu(111) and 0.13-0.14 eV for Au(111) for H-atoms that scatter from these surfaces without penetrating the surface. These energies closely correspond with energy losses predicted with Baule models, which is suggestive of structure scattering. The predicted adiabatic integral energy loss spectra (integrated over all final scattering angles) all display a lowest energy peak at an energy corresponding to approximately 80% of the average adiabatic energy loss for non-penetrative scattering. In the adiabatic limit, this suggests a way of determining the approximate average energy loss of non-penetratively scattered H-atoms from the integral energy loss spectrum of all scattered H-atoms. The AIMDEFp calculations predict that in each case the lowest energy loss peak should show additional energy loss in the range 0.2-0.3 eV due to ehp excitation, which should be possible to observe. The average non-adiabatic energy losses for non-penetrative scattering exceed the adiabatic losses to phonons by 0.9-1.0 eV. This suggests that for scattering of hyperthermal H-atoms from coinage metals the dominant energy dissipation channel should be to ehp excitation. These predictions can be tested by experiments that combine techniques for generating H-atom beams that are well resolved in translational energy and for detecting the scattered atoms with high energy-resolution. © *2014 AIP Publishing LLC*. [http://dx.doi.org/10.1063/1.4891483]

I. INTRODUCTION

The interaction of hydrogen atoms with metal surfaces is of both practical and fundamental interest. These interactions play an important role in many technologies, including hydrogen storage, nuclear fusion in tokamaks, and heterogeneous catalysis. Within the context of heterogeneous catalysis, a question of high interest is how hot atoms (HAs), which have a hot translational energy distribution that is not in equilibrium with the surface at the prevalent surface temperature (T_s), lose their energy and equilibrate to the surface. The fact that H-metal surface interactions are satisfactorily described by first principles calculations further adds to the fundamental interest of this topic.

In principle, in collisions with metal surfaces hot H atoms may lose their translational energy to the vibrations of the surface atoms ("phonons") or to the metal's electron-hole pair (ehp) excitations. The question of to what extent the energy loss proceeds adiabatically (via phonons) or non-adiabatically (via ehps) is therefore intimately connected to the question of whether the scattering of molecules and atoms

a)Electronic mail: g.j.kroes@chem.leidenuniv.nl
b)Present address: Department of Chemistry, Rutgers University, Newark, New Jersey 07102.

 © 2014 AIP Publishing LLC

This article is copyrighted as indicated in the article. Reuse of AIP content is subject to the terms at: http://scitation.aip.org/termsconditions. Downloaded to IP: 134.76.223.157 On: Thu, 18 Sep 2014 11:16:10

from metal surfaces can be accurately described within the Born-Oppenheimer approximation (BOA), a controversial hot topic in the physics and chemistry communities,[1–21] with a broad relevance to heterogeneous catalysis.[15,22–24]

For some processes, the extent to which they are affected by non-adiabaticity is now clear. For instance, purely adiabatic methods allow an accurate description of the energy exchange occurring in scattering of rare gas atoms from metal surfaces.[25] The BOA also allows an accurate description of many of the features of reactive scattering of H_2 molecules from metal surfaces.[6,10,26] In other cases, non-adiabatic effects dominate. Examples include vibrationally inelastic scattering of specific diatomic molecules from metal surfaces,[1,16,27–30] which may even be accompanied by electron emission,[5] and specific abstraction reactions.[4] Examples of special interest to H-metal interactions include vibrational lifetimes of H-atoms adsorbed to metal surfaces,[31,32] and the direct observation that collisions of H-atoms with metal surfaces may lead to ehp excitation.[3,33]

A question that has not yet received a clear answer is how strongly the translational motion of atoms and molecules interacting with metal surfaces is coupled to ehp excitation, for translational energies in the range of chemical interactions. The strength of this coupling (*T-ehp* coupling) is relevant to heterogeneous catalysis because it may determine whether an impinging atom or molecule traps at a metal surface, and thereby becomes available for reaction with another adsorbed atom or molecule, and for how long an energetic adsorbed atom produced by an exothermic surface reaction stays a HA. Important questions are whether translational energy loss processes are dominated by phonon or by ehp excitation, and to what extent the answer to the previous question depends on the mass of the incident atom or molecule, the mass of the surface atoms, and the strength of the *T-ehp* coupling. Some previous work, which has addressed a range of systems, has suggested that *T-ehp coupling* makes a negligible or minor contribution for the specific processes and systems investigated,[18,34,35] which included H-atoms interacting with Cu(110).[36] Other previous work,[37] some of which also focused on H-atoms interacting with metal surfaces,[38,39] suggested that ehp excitation should constitute the dominant energy loss mechanism.

Recent work on H-metal surface interactions has suggested that energy relaxation rates of H-atoms on metal surfaces due to phonon and ehp excitation are of similar magnitude,[19,20,40,41] but that the non-adiabatic rate is highest.[19,20,41] For instance, while Hammer and co-workers computed an energy relaxation rate due to phonon excitation of 0.7×10^{12} s^{-1} for H + Cu(111), their estimate (1.6×10^{12} s^{-1}) of the energy relaxation rate to ehp excitation from observed vibrational line widths of H adsorbed on Cu(111)[31] was larger by a factor 2.3. In very recent *ab initio* molecular dynamics calculations with electronic friction (AIMDEF calculations)[20] on HA relaxation of H-atoms resulting from dissociative chemisorption of H_2 on Pd(100), the computed energy relaxation rate to ehp excitation was a factor 5 larger than the relaxation rate to phonons. A brief account presented earlier[19] of the work we present in detail here likewise suggests that ehp excitation is the dominant energy loss channel for H-atoms scattering from Cu(111) and Au(111) at hyperthermal energies of 5 eV, although the phonons should also be important, especially for the surface consisting of the lighter atoms (Cu(111)).

The main goal of the present work is to present predictions on the basis of which experiments can determine the relative importance of energy loss to phonons and ehps in atom-metal surface scattering. We do this for what might be considered an extreme case, i.e., scattering of H atoms from Cu(111) and Au(111). These systems represent an extreme case in the sense that the mass ratio of the incident atom to the surface atom is very small (about 1/64 for Cu and about 1/197 for Au). Application of the simple Baule model[42] suggests that, if systems exist for which ehp excitation is the dominant cause of translational energy relaxation, they should be found among H-metal systems like H + Cu(111) and H + Au(111). The predictions of the energy losses we present here can in principle be tested[43] in experiments that combine methods for generating H beams of well-defined translational energy[44,45] with techniques for detecting the scattered H-atoms with high energy resolution.[44,45] If such experiments would measure translational energy losses that are substantially larger than the ones predicted with adiabatic calculations, these experiments could unambiguously attribute the excess energy losses to non-adiabatic effects. Such experimental results would be valuable as benchmark results of non-adiabatic contributions to translational energy loss, as they could serve as a testing ground for theoretical descriptions of non-adiabatic scattering from metal surfaces of atoms and molecules with energies in the range of a few eV. Another goal of our calculations is to present benchmark results that can be used to validate potential models for use in molecular dynamics (MD) simulations, which could then be used to explore a greater range of incidence conditions with better statistics and using longer simulation times than possible with AIMD.

Our choice of the H + Cu(111) system is further motivated by the fundamental interest of this system. The H_2 + Cu(111) system is a model system for activated dissociative chemisorption.[26,46–49] Scattering of H-atoms from Cu(111) is relevant to Eley-Rideal (ER) reactions, of which H + H/Cu(111) is a paradigmatic example.[50–56] We study H-atoms scattering from the model Au(111) surface because the mass ratio of H to Au is even smaller than that of H to Cu. A drawback of Au(111) is that it is known to reconstruct,[57,58] and that the resulting size of the surface unit cell is so large[57] that it makes the computational cost of *ab initio* molecular dynamics (AIMD) calculations prohibitive. However, as we will argue below, much of the results one can obtain for non-penetrative scattering of H-atoms from the model Au(111) surface are likely to be valid for non-penetrative scattering from the real (experimentally realizable) Au(111) surface. Part of this argument can be based on the findings of recent density functional theory (DFT) calculations, which suggest that the surface reconstruction only has a small influence on the interaction of surface adsorbed H-atoms with Au(111).[59] A further reason for studying H + Au(111) is that, like H + Cu(111),[60] H + Au(111) has been the subject of recent experiments that have measured ehp excitation in interactions of H-atoms with metal surfaces, and have made attempts

This article is copyrighted as indicated in the article. Reuse of AIP content is subject to the terms at: http://scitation.aip.org/termsconditions. Downloaded to IP: 134.76.223.157 On: Thu, 18 Sep 2014 11:16:10

to determine whether the observed ehp excitation could be attributed to ER or to associative desorption reactions.[60–62] Furthermore, experiments using a Schottky diode detector have detected ehp excitation in scattering of thermal H-atoms from Cu and Ag surfaces in the form of chemicurrents,[63] and such experiments have determined ehp excitation energy distributions for both thermal H- and D-atoms scattering from Ag surfaces.[64,65] Electron emission from Cu, Ag, and Au surfaces induced by hyperthermal H- and D-atoms incident in plasma beams (with energies between 15 and 200 eV) has been studied by Kovacs *et al.*[66] Much earlier, electron-hole pair excitation induced by hyperthermal Xe and Kr atoms incident on semi-conductor surfaces had been studied experimentally by Weiss *et al.*[67]

Scattering of H-atoms from copper surfaces has been investigated with electronically adiabatic models in a number of theoretical studies. Bisschler *et al.* used a soft cube model to investigate sticking, adsorption, and absorption of H-atoms on Cu(110).[36] Hammer and co-workers[41] used a potential energy surface (PES) based on semi-empirical effective medium theory and DFT calculations to study scattering of H-atoms from Cu(111) for incidence energies (E_i) ranging up to 1.2 eV and T_s up to 500 K. An important conclusion from their work was that the surface corrugation needs to be taken into account: the Baule-model fails at predicting sticking probabilities, which are affected by energy conversion from normal to parallel translational motion, and by the possibility that the H-atoms penetrate the surface even at low E_i. Klamroth and Saalfrank used reduced dimensionality quantum dynamical models, mixed-quantum classical models, and the classical trajectory method to study sticking of H-atoms from Cu(100).[68] An important conclusion of their work, which focused on methodological aspects, was that the classical mechanics results agreed well with the quantum dynamics results, while the mixed quantum-classical method did not perform so well. Shalashilin and Jackson used a restricted potential model, which did not allow surface penetration, to compute HA energy distributions and their change with time in scattering of H from Cu(111), with the aim of using the derived distributions in simulations of H_2 production through ER and HA reactions of H with H and D on Cu(111).[69] A few limited studies of H scattering from Cu(111) were performed in the wider context of the study of ER reactions, see, for instance, Ref. 52. Janke *et al.* reported preliminary results of MD simulations of H-atoms scattering from a model Au(111) surface using a PES based on effective medium theory and DFT calculations, with a focus on the applicability of the Baule model to electronically adiabatic energy transfer in single-, double-, and multiple bounce collisions.[70]

To arrive at predictions for electronically adiabatic scattering of H from Cu(111) and Au(111) that are accurate enough to attribute discrepancies with subsequent experiments unambiguously to non-adiabatic effects, it is important to account for the complexities of the scattering process that were already observed in the calculations of Hammer and co-workers[41] on H + Cu(111). These complexities include the possibility that H can experience multiple bounces on the surface through energy transfer from normal to parallel translational motion, and that H may penetrate the surface. To arrive at the required accuracy, we use AIMD,[71–73] which may be considered as the "gold standard" of high dimensional *ab initio* scattering simulations that can be performed within the framework of classical mechanics. The use of the AIMD method circumvents the need to perform high-dimensional potential fits that capture the coupling of the H-atom translational motion with the surface phonons, as forces are calculated on the fly directly from DFT. Compared to the theoretical calculations on H-atom scattering from copper and gold surfaces[36,41,68,70] that are most relevant to the present work, the research presented here uses an improved dynamical model of the phonons, avoids inaccuracies associated with potential fits, and treats a much higher E_i (5 eV) at which non-adiabatic effects should be more important. However, the computational expense of the AIMD method forces us to focus on the component of the scattering (scattering without surface penetration) that proceeds on a short time scale. Fortunately, as we will show below, experimentally it will be easiest to pick out non-adiabatic contributions to the translational energy loss for exactly this fast component. Computing statistically converged results of the adsorption probability, the absorption probability (through surface penetration), and their sum (the sticking probability) is not the goal of the present work, as performing such calculations using AIMD would be too computationally demanding at present.

The rest of this paper is organized as follows. Section II gives a summary of the methods used in our calculations. Because a detailed account of the methods used was already given in supplementary on-line material accompanying our previous short publication,[19] we will be brief and only include details that were previously omitted. Section II A describes the coordinate system we use. Section II B describes the DFT methodology also used in the AIMD calculations, and presents some results of static DFT calculations. Section II C describes the AIMD calculations. Section II D describes how we use the AIMD calculations (and in particular the trajectories of the H-atoms) to estimate the energy loss to ehp excitation, in calculations we call AIMDEFp calculations, to signify that the energy loss due to electronic friction ("EF") is computed after ("p" for "post") the AIMD dynamics is done. This differs from the method that is used in the very recently introduced AIMDEF method,[20] where the instantaneous effect of electronic friction is incorporated in the computation of the actual trajectory. Section II E describes the statistical method we use to show that, for incidence conditions with $\phi_i = 0^\circ$ (see Fig. 1 and Sec. II A), the polar angular distributions for ϕ_f and $-\phi_f$ are different. These differences are interesting because they show that scattering of hyperthermal H-atoms from (111) surfaces of face centered cubic (FCC) metals may probe the subsurface region of the metal, in principle leading to recognizable differences between the interactions of H with fcc and hcp sites.

Section III presents the results of our calculations, which were all done for $E_i = 5$ eV. Predictions are presented for scattering of H-atoms from Cu(111) and a model Au(111) surface at a polar incidence angle $\theta_i = 15^\circ$, and for incidence along the $[11\bar{2}]$ direction (see Fig. 1). For H + Au(111), we also present predictions for scattering at a different polar incidence angle ($\theta_i = 60^\circ$), and for a different incidence di-

This article is copyrighted as indicated in the article. Reuse of AIP content is subject to the terms at: http://scitation.aip.org/termsconditions. Downloaded to IP: 134.76.223.157 On: Thu, 18 Sep 2014 11:16:10

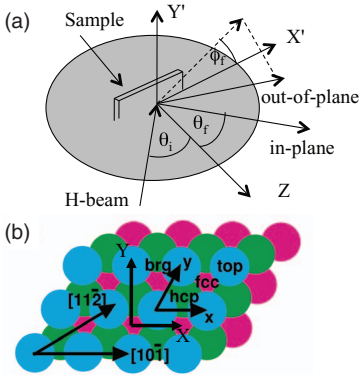

FIG. 1. Definition of incidence angle θ_i, and scattering angles θ_f and ϕ_f (a). Plot of the (111) surface of FCC metals such as Cu and Au (b). Indicated are the high symmetry sites top, hcp, fcc, and bridge (brg). Also indicated are the crystallographic directions corresponding to the two planes of incidence studied in this work.

rection (the [10$\bar{1}$] direction). Results are presented regarding the probabilities of different scattering outcomes (Sec. III A), adiabatic energy loss distributions (Sec. III B), angular distributions (Sec. III C), and non-adiabatic energy loss distributions (Sec. III D). Our earlier and much shorter publication[19] focused on identifying conditions at which atoms scattering without penetration of the surface can be measured on H + Au(111) for one particular incidence condition, and on AIMD results. Part of the results presented earlier[19] also occur in the present work, which presents a more complete picture. Compared to the earlier work, far more results are presented for H + Cu(111), and for H + Au(111) at another incidence condition. We also present much more detailed angular distributions, and investigate the correlation between the angularly resolved energy loss distributions and the angular distributions of the atoms scattering with and without penetration. Finally, results of the non-adiabatic (AIMDEFp) calculations are presented and discussed in far greater detail than was possible in Ref. 19.

Discussion is provided in Sec. IV. Section IV A discusses the scattering probabilities computed with AIMD, Sec. IV B the energy loss to phonons predicted with our AIMD calculations, and Sec. IV C energy loss to ehps. In Sec. IV D we discuss the angular scattering distributions predicted with AIMD, and in Sec. IV E the possibility of experimentally probing the subsurface region of (111) surfaces of FCC metals with hyperthermal H-atoms. Section IV F discusses possible directions for future research, and these are summarized along with the conclusions in Sec. V.

II. METHOD

A. Coordinate system

The conventions adopted for the incidence angle θ_i and the scattering angles θ_f and ϕ_f are illustrated in Fig. 1(a), and the structure of the (111) surface of a FCC metal (like copper and gold) is shown in Fig. 1(b). Fig. 1(b) also displays the high symmetry sites top (first layer atom), hcp (the hollow site above a second layer atom), fcc (the hollow site above a third layer atom), and bridge (brg, a site midway between two neighboring top sites). In a FCC metal atoms in the fourth layer are beneath atoms in the first layer. The "t2h" ("t2f") sites are midway between neighboring top and hcp (fcc) sites.

We use two Cartesian coordinate systems, i.e., a lab frame and a reference frame. In the right-handed lab frame coordinate system, the Z-axis is the surface normal, pointing away from the surface. The X-axis is in the [10$\bar{1}$] crystallographic direction (Fig. 1(b)). The polar angle of incidence θ_i and the polar scattering angle θ_f are defined relative to this coordinate system (Fig. 1(a)). Furthermore, we follow an often used convention in surface *science* in which both polar angles are taken in the range [0°,90°] (Fig. 1(a)). Both angles are defined relative to the Z-axis, and $\theta_i = 0°$ denotes incidence normal to the surface.

The azimuthal incidence angle ϕ_i describes the orientation of the incidence plane relative to the lab frame: the reference frame is the right-handed coordinate system X′Y′Z in which the incident H atom moves in the X′Z plane, in the positive X′ direction. The X′ and Y′ axes can be obtained by rotating the X and Y axes counter-clockwise around the Z-axis over an angle ϕ_i. Incidence along the [10$\bar{1}$] direction means $\phi_i = 0°$, and for $\phi_i = 30°$, incidence is in the [11$\bar{2}$] direction (see Fig. 1(b)). The Y-axis should not be confused with the y-axis in Fig. 1(b), which makes an angle of 60° with the x-axis also defined in Fig. 1(b).

The azimuthal scattering angle ϕ_f (see Fig. 1(a)) is referenced to the particular incidence direction considered, which is described by ϕ_i, and ϕ_f takes on values between −180° and 180°. With these definitions $\phi_f = 0°$ describes forward in-plane scattering, with specular scattering occurring for $\phi_f = 0°$ and $\theta_f = \theta_i$, $\phi_f = 180°$ describes backward in-plane scattering, and $\phi_f = 90°$ side-ways scattering. For $\phi_i = (30° \pm n\,60°)$ the scattering distributions for the final scattering angles $+\phi_f$ and $-\phi_f$ are equal by symmetry, but they are expected to differ for $\phi_i = (0° \pm n\,60°)$. The Cartesian components of the initial and final velocities $\vec{v}_i$ and $\vec{v}_f$ may be written in terms of the total initial and final velocities and the coordinates introduced here as detailed in the supporting information to Ref. 19.

B. DFT calculations

To obtain energies and forces, DFT[74,75] calculations were carried out with a modified version of the VASP code.[76–79] The exchange-correlation energy of the electrons is described at the generalized gradient approximation (GGA) level. We have used the SRP48 functional,[49] which has been designed to reproduce reactive scattering experiments on H_2 + Cu(111),[49] and which has been shown to be transferable to the H_2 + Cu(100) system.[80] For the sake of consistency and for reasons explained further in Ref. 19 we therefore also use this functional for H + Cu(111), and for H + Au(111).

With a view to mapping out potential curves, we carried out static (single-point) DFT calculations on H + Cu(111) and Au(111). The metal atoms were kept frozen at their positions in the relaxed bare metal slab,[19] but the position of the H-atom was varied in these calculations. In the supercell approach employed, a four-layer metal (Cu or Au) slab and a (2×2) surface unit cell were used to model the adsorbate/substrate system,

This article is copyrighted as indicated in the article. Reuse of AIP content is subject to the terms at: http://scitation.aip.org/termsconditions. Downloaded to IP: 134.76.223.157 On: Thu, 18 Sep 2014 11:16:10

and a vacuum layer of 13.0 Å was placed between the slabs in the Z direction. To sample the Brillouin zone an $8\times8\times1$ grid of shifted (Γ-centered) Monkhorst-Pack *k*-points[81] was used. A cut-off energy of 350 eV was used in the plane-wave expansion, and a Fermi level smearing of 0.1 eV to facilitate convergence. Depending on the distance of the atom to the surface, spin-unpolarized or spin-polarized calculations were done as detailed in Ref. 19. We estimate that our H-atom surface interaction energies are converged to within approximately 60 meV with respect to the input parameters discussed above.

Potential curves (Fig. 2) were computed for H being above or below the top, bridge, fcc hollow, hcp hollow, and t2f and t2h sites (see also Fig. 1). The potential minima were found for H being above the fcc site and above the surface. The comparison of the computed minimum interaction energy with other calculated and with experimental values is discussed in Ref. 19. We note that H-atoms incident from the gas phase may penetrate the surface without barrier (taking the gas phase energy as reference) for impact on the bridge, fcc, and hcp sites. We also note that the interaction of H with Cu(111) is qualitatively quite similar to the interaction of H with Au(111), and that for both metals the interaction of H with the fcc (t2f) site only starts to differ markedly from the interaction with the hcp (t2h) site once the atom drops below the first layer (for $Z < 0$ Å).

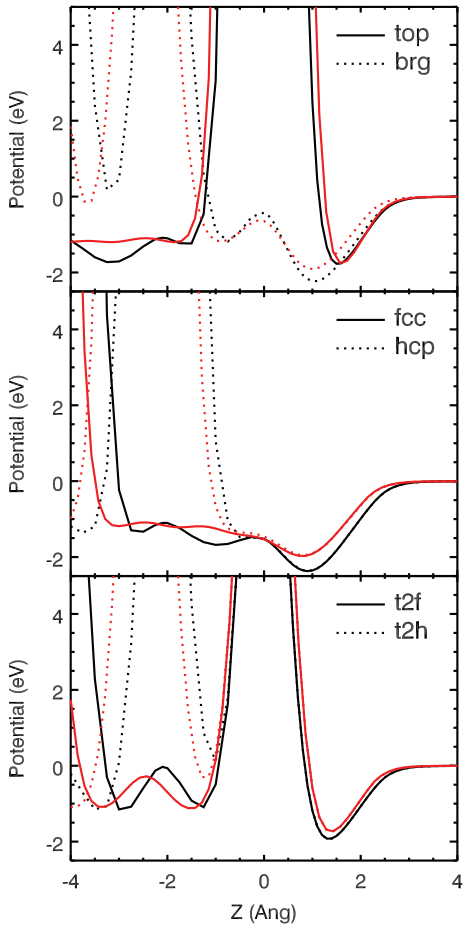

FIG. 2. The H-surface interaction potential is shown as a function of the atom-surface distance Z in Å, for H + Cu(111) (black lines) and H + Au(111) (red or gray lines, see also Fig. 1 and Sec. II A for the sites). Data taken from Ref. 19.

Recent DFT calculations suggest that the interaction of H with Au(111) should be increased if the experimentally found[82–84] herringbone reconstruction of Au(111) is taken into account.[59] Specifically, by modeling only the straight sections in the herringbone reconstruction it was found that the well depth increased by values in the range 53-65 meV.[59] It is possible that an even larger interaction would be found at the so-called elbow sites where the straight sections ("stripes") of the reconstructed surface meet, making an angle of 120° with one another (see, for instance, Figure 1(b) of Ref. 59).

C. *Ab initio* molecular dynamics calculations

In the AIMD method[71–73,85–88] used here, dynamical quantities are computed using classical Born-Oppenheimer dynamics for nuclear motion while computing the forces on the fly using DFT. The Cu (Au) substrate was modeled using 4 layers as in the static surface calculations discussed above. More generally, all input parameters to the electronic structure part of VASP were taken the same as discussed above. Only the upper 3 layers were allowed to move, with the bottom layer of atoms kept fixed. Molecular dynamics simulations were performed in the NVE ensemble (i.e., keeping the number of particles N, the volume V, and the total energy E fixed), employing the Verlet algorithm.[89,90] A value of 120 K was imposed on the T_s of the Cu and Au surfaces as discussed in Ref. 19.

In the scattering AIMD calculations on H + Cu(111) and Au(111), we used the classical trajectory (CT) method,[91] i.e., classical molecular dynamics with Monte-Carlo sampling of the initial conditions. For the metal, E_i (5 eV in all calculations), θ_i, and incidence plane selected scattering probabilities are calculated as detailed in Ref. 19. Depending on the distance of H to the surface and on whether H moved towards or away from the surface, the AIMD calculations were done using spin-polarized or spin-unpolarized DFT, and performed in multi-step or single-step mode, as detailed in Ref. 19.

The procedure used is as follows. The H-atom trajectories are started at 6.0 Å above the surface. The maximum propagation time used is 120 fs (to avoid artifacts associated with the heat wave generated by the collision, for instance, its reflection from the static metal layer at the bottom[19]), and the time step 0.1 fs. A collision is assigned the outcome "scattering" whenever the atom bounces back to the gas phase and reaches a distance from the surface >6.1 Å (the trajectory is then stopped). A trajectory is also labeled "scattering" if after 120 fs the H-atom is moving away from the surface at $Z \geq 3.3$ Å, and its normal kinetic energy exceeds the H-static Me(111) surface interaction averaged over the top, bridge, fcc, hcp, t2f, and t2h sites by 50 meV at the current value of Z. Trajectories in which the H-atoms fly through the 4-layer slab to emerge at the other end are called "fly through." The outcome of trajectories that fall in neither of these two categories is classified as "unclear." The scattered trajectories were further subdivided. We distinguish[19] between trajectories in which the H-atoms scatter from the surface without and with entering the subsurface, where in the latter case the leaving H subsequently re-emerges at the gas phase side (scattering without and with

This article is copyrighted as indicated in the article. Reuse of AIP content is subject to the terms at: http://scitation.aip.org/termsconditions. Downloaded to IP: 134.76.223.157 On: Thu, 18 Sep 2014 11:16:10

penetration). We also distinguish between direct and indirect scattering trajectories. In a direct (indirect) scattering trajectory, the Z-value of the H-atom exhibits one (multiple) inner turning point(s).

In our calculations the probability p_e of an event is simply computed as the ratio (N_e/N_t) of the number of times the event occurred (N_e) divided by the total number of trajectories $(N_t = 900)$. Standard errors defining 68% confidence intervals are computed from $s = \sqrt{p_e(1-p_e)/N_t}$. For good statistics, distributions of the adiabatic energy loss to phonons, ΔE, integrated over all scattering angles are computed with large bin widths (50 meV for H + Cu, and 25 meV for H + Au). Energy loss distributions computed for one final solid angle are computed with even larger bin widths (400 meV for H + Cu, 200 meV for H + Au). Angular distributions are computed with large and overlapping bin widths, using $\Delta\phi_f = 60^\circ$ and $\Delta\theta_f = 15^\circ$. In the computation of angular distributions the statistics was further improved for calculations in which incidence was along a symmetry plane by adding a trajectory scattering with $(\theta_f, -\phi_f)$ for each trajectory scattered to (θ_f, ϕ_f).

D. *Ab initio* molecular dynamics with electronic friction calculations

We have also used our AIMD results and friction theory to estimate the non-adiabatic energy loss, ΔE_{NA}, which is the sum of the energy loss to phonons and to ehp excitation. For each trajectory, ΔE_{NA} for a particular H-atom surface collision was calculated after the entire trajectory was computed with ordinary AIMD, i.e., the energy loss resulting from the friction force was calculated "post" the trajectory. For this reason we call the calculations we performed "AIMDEFp calculations." An even better approach would have been to apply the friction force on the H-atom while it is moving in what are called AIMDEF calculations, as suggested in Ref. 92. However, this approach only became available[20] after the AIMD calculations presented here were already done. Instead, we used the time-dependent H-atom coordinates $\vec{r}(t)$ and velocities $\vec{v}(t)$ from the AIMD trajectories and electronic friction coefficients to compute the energy loss due to ehp excitation. Using a position-dependent friction coefficient, $\eta(\vec{r})$, the energy loss to ehp excitations incurred during the time t_c that the H-atom interacts with the surface was computed as

$$E_{NA} = \int_{t=0}^{t_c} \eta(\vec{r}(t))v(t)^2 dt. \quad (1)$$

The total non-adiabatic energy loss to the surface, ΔE_{NA}, can then be calculated as the sum of the adiabatic energy loss to the phonons, ΔE, and ΔE_{NA}^{eh}.

The friction coefficients were computed within the local density friction approximation (LDFA).[10] This approach assumes that, at a particular point $\boldsymbol{r}$ on or in a metal surface where the bare surface has a specific electron density, the friction coefficient of an atom interacting with that metal can be taken the same as that of the same atom in a free electron gas of the same density. Friction coefficients computed within the LDFA have previously been successfully applied to understand different properties of the energy loss of atoms and ions on surfaces.[93–96] Here, an additional approximation made was that the electronic density was calculated fixing the metal atoms at their equilibrium positions at $T_s = 120$ K.

Friction coefficients may also be computed using different approaches, and we have previously compared[19] LDFA friction coefficients for the H-atom approaching Cu(111) above a first-layer surface atom with friction coefficients computed by Trail *et al.*[40] for the same system and approach geometry, but using a different method. The comparison suggested that energy losses that would be calculated for the systems and conditions considered here using the alternative theory for computing friction coefficients of Ref. 40 should be similar to or greater than the non-adiabatic energy losses calculated here.

E. Statistical method for detecting significant differences between angular distributions

For incidence along the $[10\bar{1}]$ direction ($\phi_i = 0^\circ$), scattering distributions in θ_f are expected to differ for the final scattering angles ϕ_f and $-\phi_f$, because the $[10\bar{1}]$ plane is not a symmetry plane. To determine whether calculated differences between angular distributions are statistically significant, the Pearson χ^2 statistic can be calculated using

$$\chi^2 = \sum_{j=1}^{J} \frac{(f_{oj} - f_{ej})^2}{f_{ej}}. \quad (2)$$

In Eq. (2), f_{ej} is an "expected frequency," f_{oj} is an "observed frequency," and J is the number of distinct categories (solid angle regions) in which scattered trajectories are binned, so that $\nu = J$-1 is the number of degrees of freedom of the associated test of the null hypothesis:

H_0: the polar angular distributions are identical for ϕ_f and $-\phi_f$

Two types of angular distributions can be compared. In the most comprehensive comparison, the number of atoms scattered to solid angle regions $(\theta_j, 360^\circ\text{-}\phi_j)$ (observed frequencies) are compared to the number of atoms scattered to solid angle regions (θ_j,ϕ_j) (expected frequencies) with summing over both θ and ϕ. Here, the "observations" have been carried out for $\theta = 7.5^\circ$, 22.5°, 37.5°, 52.5°, 67.5°, and 82.5°, and $\phi = 30^\circ$, 90°, and 150°, and to ensure that all observations were included the category $\phi > 180^\circ$ ($\phi < 180^\circ$) was added to the categories for which the expected (observed) frequencies were computed, so that $J = 19$. In the second type of comparison, the number of atoms scattered to solid angle regions $(\theta_j,360^\circ\text{-}\phi_t)$ (observed frequencies) are compared to the number of atoms scattered to solid angle regions (θ_j,ϕ_t) (expected frequencies) with summing over θ only, for a fixed value of ϕ_t, and using the same values of θ. Such tests were carried out for $\phi_t = 30^\circ$, 60°, 90°, 120°, and 150°. To ensure that all observations were included the category $\phi \neq \phi_t$ ($\phi \neq 360^\circ\text{-}\phi_t$) was added to the categories for which the expected (observed) frequencies were computed, so that $J = 7$. The so-called p-value is the probability that the null

This article is copyrighted as indicated in the article. Reuse of AIP content is subject to the terms at: http://scitation.aip.org/termsconditions. Downloaded to IP: 134.76.223.157 On: Thu, 18 Sep 2014 11:16:10

hypothesis is rejected even though it is true. In a statistical test, one rejects the null hypothesis (and typically accepts an alternative hypothesis) if the p-value falls below a predefined confidence level α (often taken as 0.05, i.e., 5%, but here we also report results for $\alpha = 0.1$ (10%) in view of the limited number of AIMD trajectories we were able to run).

III. RESULTS

A. Scattering outcomes

Probabilities of scattering outcomes are presented in Tables I and II. The probability of scattering of H from Cu(111) at $E_i = 5$ eV, $\theta_i = 15°$, and incidence along the $[11\bar{2}]$ direction ($\phi_i = 30°$, see Fig. 1) is 58%. The probability of scattering of H from Au(111) under the same incidence conditions is 66%, while the scattering probability is greatest (72%) for incidence along the $[10\bar{1}]$ direction ($\phi_i = 0°$) with $\theta_i = 60°$. The interpretation of the remainder of the trajectories is unresolved due to the limited propagation time and the finite thickness of the metal slabs modeled. For instance, for H incident on Cu(111), 16% of the H-atoms fly through the 4-layer slab, and 26% have an unclear outcome (Table I, which also gives results for the two other systems).

Focusing on the H-atom collisions that lead to an unclear outcome, we find that after 120 fs most of the H-atoms associated with this outcome have penetrated the metal slab. For instance, for H + Cu(111) among the 26% H-atoms with an unclear outcome 2.9% had not yet and 23.3% had penetrated the surface. For H + Cu(111) our results may therefore be considered accurate for non-penetrative scattering: the associated probability should be between 30% and 33% (Table II), so that a maximum of 9% is missing from the batch of trajectories that could scatter without penetration. A similar analysis performed for H + Au(111) leads to the same conclusion for both incidence conditions investigated, with a maximum of 6% missing from the trajectories that could scatter without penetration for ($\theta_i = 15°$, $\phi_i = 30°$) and a maximum of 9.5% missing for ($\theta_i = 60°$, $\phi_i = 0°$).

We now consider the accuracy of our approach for penetrative scattering. For H + Cu(111), the associated probability lies between 28% (the result after 120 fs propagation using a 4 layer slab) and 70% (considering that all unclear and fly through trajectories might scatter with penetration in a long-time simulation using a thicker copper slab, see Table II). Therefore, for H + Cu(111) we may have analyzed only 40% of the H-atoms that could scatter with penetration, so that other results for this category of scattered H-atoms (such as the average energy loss to the surface) might not be accurate either. A similar analysis applies for H + Au(111). For instance, a similar analysis applied to the data present in Table II shows that we may have analyzed only 46% of the H-atoms that could scatter with penetration for ($\theta_i = 15°$, $\phi_i = 30°$) and only 34% for ($\theta_i = 60°$, $\phi_i = 0°$). Considering these results, we expect that for all systems investigated the average calculated energy loss, $\langle E \rangle$, of the atoms that scatter with penetration may well be too low, because we miss the contribution of the atoms that could scatter after staying in the slab for a longer time, or by bouncing back from a deeper surface layer than simulated here. For H + Au(111) we

TABLE I. Probabilities (p), adiabatic energy losses (ΔE) calculated with AIMD, and non-adiabatic energy losses (ΔE_{NA}) calculated with AIMDEFp associated with several scattering events, for H + Cu(111) and $\theta_i = 15°$ and $\phi_i = 30°$, H + Au(111) and $\theta_i = 15°$ and $\phi_i = 30°$, and H + Au(111) and $\theta_i = 60°$ and $\phi_i = 0°$. Part of the data contained in the table have been published earlier in Ref. 19.

Quantity	Cu(111), $\theta_i = 15°$, $\phi_i = 30°$	Au(111), $\theta_i = 15°$, $\phi_i = 30°$	Au(111), $\theta_i = 60°$, $\phi_i = 0°$
Scattering probability	0.583 ± 0.016	0.657 ± 0.016	0.723 ± 0.015
ΔE (eV)	0.88 ± 0.03	0.29 ± 0.01	0.21 ± 0.01
ΔE_{NA} (eV)	2.49 ± 0.07	1.93 ± 0.06	1.52 ± 0.04
Scattering probability, with penetration	0.282 ± 0.015	0.289 ± 0.015	0.140 ± 0.012
ΔE (eV)	1.41 ± 0.05	0.49 ± 0.02	0.51 ± 0.02
ΔE_{NA} (eV)	3.75 ± 0.10	3.06 ± 0.09	3.09 ± 0.09
Scattering probability, without penetration	0.301 ± 0.015	0.377 ± 0.016	0.583 ± 0.016
ΔE (eV)	0.38 ± 0.01	0.13 ± 0.01	0.14 ± 0.01
ΔE_{NA} (eV)	1.32 ± 0.05	1.04 ± 0.04	1.14 ± 0.03
Direct scattering p, without penetration	0.212 ± 0.014	0.258 ± 0.015	0.427 ± 0.016
ΔE (eV)	0.34 ± 0.01	0.11 ± 0.01	0.13 ± 0.01
ΔE_{NA} (eV)	0.93 ± 0.03	0.69 ± 0.02	0.96 ± 0.02
Indirect scattering P, without penetration	0.089 ± 0.009	0.110 ± 0.010	0.157 ± 0.012
ΔE (eV)	0.49 ± 0.02	0.15 ± 0.01	0.16 ± 0.01
ΔE_{NA} (eV)	2.23 ± 0.07	1.88 ± 0.07	1.89 ± 0.05
Fly through probability	0.155 ± 0.012	0.148 ± 0.012	0.073 ± 0.009
Unclear probability (after 120 fs)	0.262 ± 0.015	0.196 ± 0.013	0.203 ± 0.013

This article is copyrighted as indicated in the article. Reuse of AIP content is subject to the terms at: http://scitation.aip.org/termsconditions. Downloaded to IP: 134.76.223.157 On: Thu, 18 Sep 2014 11:16:10

TABLE II. Probabilities (p) associated with several scattering events calculated with AIMD, for H + Cu(111) and $\theta_i = 15^\circ$ and $\phi_i = 30^\circ$, H + Au(111) and $\theta_i = 15^\circ$ and $\phi_i = 30^\circ$, and H + Au(111) and $\theta_i = 60^\circ$ and $\phi_i = 0^\circ$. The probability of scattering with penetration is decomposed into three contributions according to the number of layers penetrated by the H atom. The probability p(120 fs) is computed after 120 fs as described in Sec. II. The other probabilities are upper bounds that would be obtained in an infinitely long simulation, ignoring errors due to the truncation of the slab at 4 layers. To calculate the upper bound in method A, we assume that all H-atoms which end up in the slab below layer n will next proceed to scatter back to the gas phase, without further penetration of layers below. In method B, we also assume that all H-atoms in the slab will desorb, but we take in to account that atoms above layer n may still go deeper before they emerge. Part of the data contained in the table have been published earlier in Ref. 19.

Event	Cu(111), $\theta_i = 15^\circ$, $\phi_i = 30^\circ$	Au(111), $\theta_i = 15^\circ$, $\phi_i = 30^\circ$	Au(111), $\theta_i = 60^\circ$, $\phi_i = 0^\circ$
Scattering with penetration, p(120 fs)	0.282 ± 0.015	0.289 ± 0.015	0.140 ± 0.012
$p(t = \infty)$ A	0.67	0.61	0.35
$p(t = \infty)$ B	0.70	0.63	0.42
Scattering without penetration, p(120 fs)	0.301 ± 0.015	0.377 ± 0.016	0.583 ± 0.016
$p(t = \infty)$ A	0.33	0.40	0.64
$p(t = \infty)$ B	0.33	0.40	0.64
Scattering with pen. of 1 layer, p(120 fs)	0.179 ± 0.013	0.209 ± 0.014	0.113 ± 0.001
$p(t = \infty)$ A	0.23	0.23	0.14
$p(t = \infty)$ B	0.26	0.25	0.21
Scattering with pen. of 2 layers, p(120 fs)	0.098 ± 0.010	0.070 ± 0.009	0.024 ± 0.005
$p(t = \infty)$ A	0.19	0.14	0.10
$p(t = \infty)$ B	0.27	0.18	0.19
Scattering with pen. of 3 layers, p(120 fs)	0.006 ± 0.002	0.010 ± 0.003	0.002 ± 0.002
$p(t = \infty)$ A	0.10	0.09	0.04
$p(t = \infty)$ B	0.27	0.21	0.21

additionally note that while the probabilities given above can be useful in comparisons with future calculations considering scattering of H from the model Au(111) surface, one should keep in mind that experiments will probe the herringbone reconstructed Au(111) surface,[59] and therefore the experimental probability of scattering with penetration might differ.

In contrast to the broader category of H-atoms that scatter penetratively, the fraction of atoms that scatter with penetration of only one surface layer is rather well determined for incidence with ($\theta_i = 15^\circ$, $\phi_i = 30^\circ$). For instance, for H + Cu(111) this fraction is in the range 18%–26%, and for H + Au(111) this fraction is 21%–25%. (Table II). The reason is that for this incidence condition many of the "unclear atoms" have already penetrated the second surface layer. In contrast to the other incidence condition for both Cu and Au, the fraction of atoms that scatter from the model Au(111) surface at $\theta_i = 60^\circ$, and $\phi_i = 0^\circ$ with penetration of only one surface layer is less well defined, falling between 11% and 21% (Table II). The larger uncertainty in this number comes from the possibilities that atoms lingering above the surface (6%) and below layer 1 but above layer 2 (4%) might still return to the gas phase after penetrating only one layer. The probability that the atoms scatter with penetration of two or more surface layers becomes progressively more uncertain as the number of layers increases for all systems investigated (Table II).

B. Adiabatic energy loss

The adiabatic ΔE distribution integrated over all scattering angles (i.e., the integral ΔE distribution) is shown in Figs. 3(a)–3(c) for the three systems investigated. In all cases a wide energy loss distribution is observed, although the distributions are narrower for Au than for Cu. The atoms that scatter without penetration from Cu(111) on average lose 0.38 eV to the surface (Table I), with the standard deviation σ characterizing the distribution being 0.18 eV. In contrast, atoms scattering without penetration from Au(111) only lose 0.13 eV (0.14 eV) to the surface (Table I) with a with a σ-value of 0.09 eV (0.11 eV), for $\theta_i = 15^\circ$ and $\phi_i = 30^\circ$ ($\theta_i = 60^\circ$ and $\phi_i = 0^\circ$). The atoms that scatter penetratively on average lose much more energy to the surface, and show a much wider ΔE distribution than the atoms scattered without penetration. For instance, H-atoms scattering penetratively from Cu(111) lose 1.41 eV to the surface (Table I, which also shows values for the other 2 systems), with a standard deviation of 0.75 eV. The average ΔE of all scattered H-atoms is 0.88 eV for Cu(111) (Table I, $\sigma = 0.74$ eV), 0.29 eV for Au, and $\theta_i = 15^\circ$ and $\phi_i = 30^\circ$, and 0.21 eV for Au and $\theta_i = 60^\circ$ and $\phi_i = 0^\circ$. As mentioned in Sec. III A, the $\langle \Delta E \rangle$ of the atoms scattered with penetration is probably underestimated, and the $\langle \Delta E \rangle$ of all scattered atoms should be underestimated for the same reasons. The $\langle \Delta E \rangle$ of the atoms scattered without penetration is based on >90% of the relevant trajectories and thus should be more accurate for all systems investigated.

In the adiabatic picture, all atoms that scattered with penetration of the Cu(111) surface lost at least 0.3 eV of energy to the surface (Fig. 3(a)). All atoms that lose less energy to Cu(111) have scattered without penetration. Because our approach should give accurate results for this category of atoms, the energy loss distribution in Fig. 3(a) should

This article is copyrighted as indicated in the article. Reuse of AIP content is subject to the terms at: http://scitation.aip.org/termsconditions. Downloaded to IP: 134.76.223.157 On: Thu, 18 Sep 2014 11:16:10

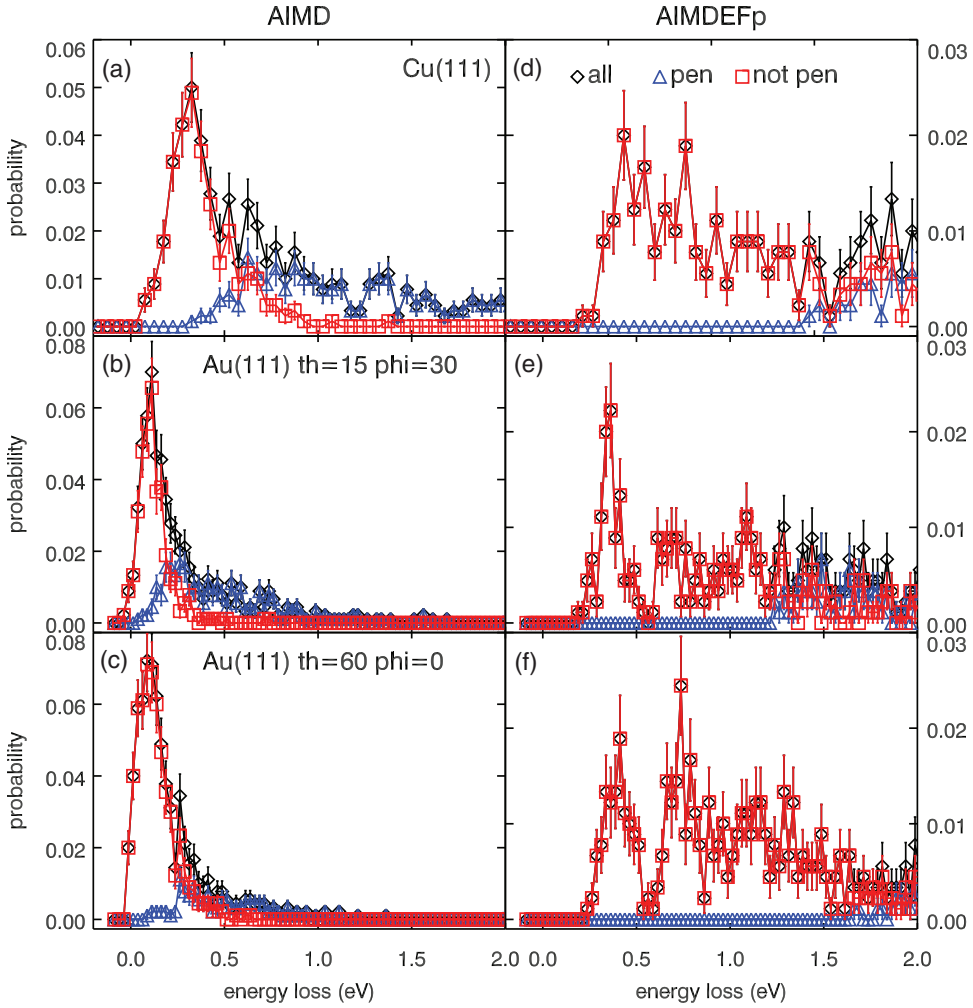

FIG. 3. The integral adiabatic (a–c) and non-adiabatic (d–f) energy loss distributions are shown of H-atoms that have scattered from the surface (all), that have scattered from the surface with penetration (pen), and that have scattered from the surface without penetration (not pen, see inset to panel d). Results are shown for $E_i = 5$ eV, for $\theta_i = 15^\circ$ and $\phi_i = 30^\circ$ for H + Cu(111) (a, d) and H + Au(111) (b, e) and for $\theta_i = 60^\circ$ and $\phi_i = 0^\circ$, for H + Au(111) (c,f). Data in panels (d–f), and data in panels (a–c) for ΔE up to 1 eV, were taken from Ref. 19.

constitute an accurate adiabatic dynamics prediction for ΔE up to 0.3 eV. Inspection of Figs. 3(b) and 3(c) shows that, for H + Au(111), the same should be true for ΔE up to 25 meV for $\theta_i = 15^\circ$ and $\phi_i = 30^\circ$, and for ΔE up to 75 meV for $\theta_i = 60^\circ$ and $\phi_i = 0^\circ$. These results suggest that it should be easiest to distinguish atoms scattering without penetration by measuring integral energy loss spectra for Cu, while for Au it should be easier to distinguish atoms scattering without penetration for the incidence condition $\theta_i = 60^\circ$ and $\phi_i = 0^\circ$ than for $\theta_i = 15^\circ$ and $\phi_i = 30^\circ$. For all cases studied penetrative scattering leads to a considerable broadening of the distribution of the energy loss of all scattered H-atoms. The resulting broadening contribution may well be underestimated in our present results as we may have analyzed only a small fraction of the atoms that scatter with penetration for all systems investigated (see Sec. III A). Regarding the accuracy of our predicted energy loss distributions, for H + Au(111) we note once more that the calculations were done for a model Au(111) surface while experimentally the surface reconstructs, and it is likely that this difference affects the energy loss distribution for atoms scattering penetratively.

Of the atoms scattered without penetration, for H + Cu(111) approximately 70% do so directly (see Sec. II C), while the remaining trajectories scatter indirectly, and similar percentages apply to H + Au(111) for the two incidence conditions investigated (see Table I). As might be expected, the directly scattered atoms on average lose less energy (0.34 eV) than the ones scattered with multiple bounces (0.49 eV, see Table I), and a similar conclusion applies to H + Au(111) (Table I). The category of atoms that scatters indirectly but without penetration contributes to a broadening of the energy loss distributions of all scattered atoms, but to a much smaller extent than the atoms that scatter penetratively.

C. Adiabatic angular distributions

The angular distribution of the scattered H-atoms is extremely broad, and this is true for both atoms that scatter with and without penetration, as observed for H + Cu (Fig. 4) and for H + Au(111) for both incidence conditions investigated (Figs. 5 and 6). For H + Au(111) and $\theta_i = 60^\circ$ and $\phi_i = 0^\circ$

This article is copyrighted as indicated in the article. Reuse of AIP content is subject to the terms at: http://scitation.aip.org/termsconditions. Downloaded to IP: 134.76.223.157 On: Thu, 18 Sep 2014 11:16:10

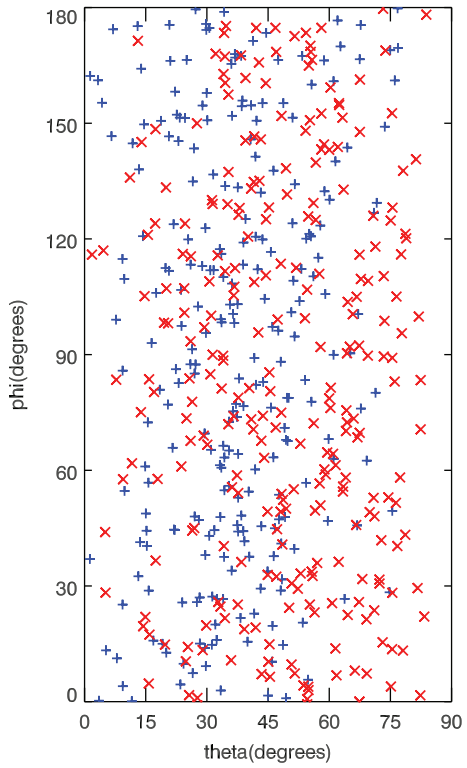

FIG. 4. Angular distribution of H-atoms scattering from Cu(111) for $\theta_i = 15^\circ$ and $\phi_i = 30^\circ$ with (blue plus symbols) and without penetration of the surface (red crosses).

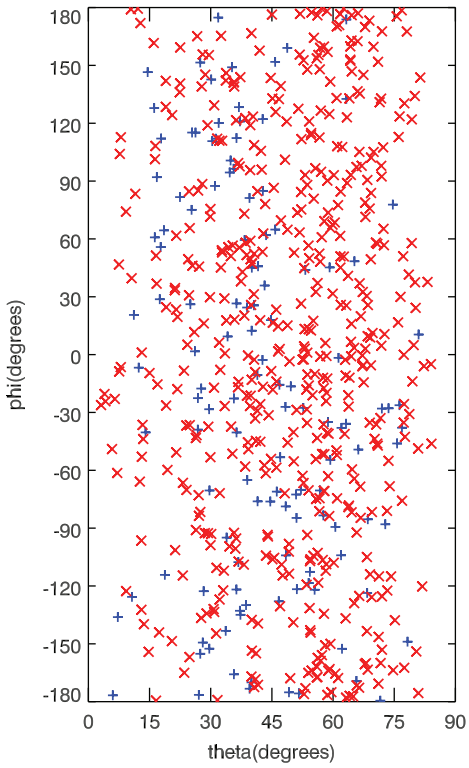

FIG. 6. Angular distribution of H-atoms scattering from Au(111) at incidence angles $\theta_i = 60^\circ$ and $\phi_i = 0^\circ$, with (blue plus symbols) and without penetration of the surface (red crosses).

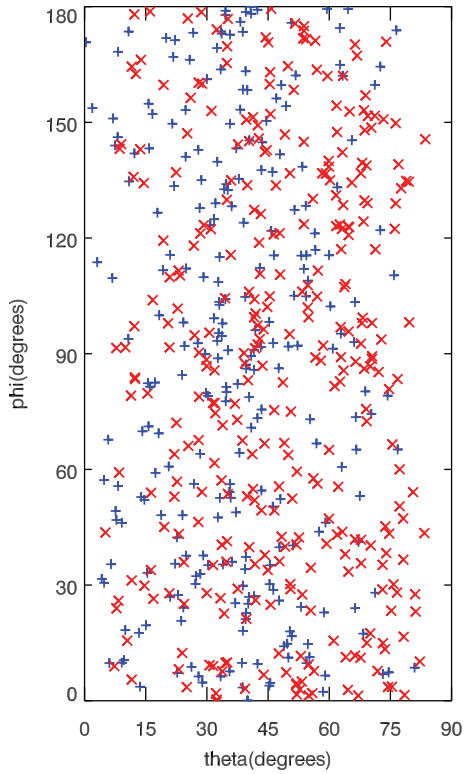

FIG. 5. Angular distribution of H-atoms scattering from Au(111) at incidence angles $\theta_i = 15^\circ$ and $\phi_i = 30^\circ$, with (blue plus symbols) and without penetration of the surface (red crosses).

the angular distribution is plotted over the range $-180^\circ < \phi_f \leq 180^\circ$ because the plane of incidence that slices through the surface atoms is no longer a reflection plane, so that scattering is expected to be different for ϕ_f and $-\phi_f$ (Fig. 6).

In spite of the broadness of the angular distributions of both categories of scattered atoms (with and without penetration), there are solid angle regions to which no or hardly any atoms scatter with penetration. For instance, for Cu the angular distribution for forward in-plane scattering shows no penetrative scattering with $\theta_f = 82.5^\circ$, and very little penetrative scattering with $\theta_f = 75.0^\circ$ (Fig. 7(a)). Furthermore, the angularly resolved ΔE distribution (Fig. 7(b)) suggests that it should be possible to resolve the contributions of atoms that scatter to these angles with and without penetration by measuring their final translational energy, with the atoms scattered with penetration losing much more energy (Fig. 8).

Solid angles to which H-atoms scatter (almost) exclusively without penetration are of special interest to experiments aiming to determine whether the scattering occurs with large losses to ehp excitation: for these solid angles, the nonadiabatic contribution to the energy loss should stand out because little energy is lost to phonons. We have therefore also investigated whether such solid angle regions could be identified for H + Au(111). For $\theta_i = 15^\circ$ and $\phi_i = 30^\circ$, we found no solid angle regions to which no atoms scatter with penetration, but we did find regions to which only few atoms scatter with penetration. For instance, the angular distribution for forward in-plane scattering shows little penetrative scattering with $\theta_f = 75.0^\circ$ (Fig. 9(a), note that the same is true for H + Cu and

This article is copyrighted as indicated in the article. Reuse of AIP content is subject to the terms at: http://scitation.aip.org/termsconditions. Downloaded to IP: 134.76.223.157 On: Thu, 18 Sep 2014 11:16:10

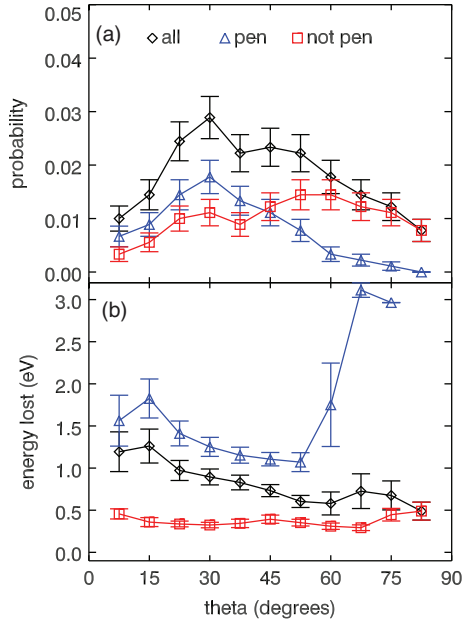

FIG. 7. Angular[19] and energy loss distribution of H-atoms scattering from Cu(111) for $\theta_i = 15°$ and $\phi_i = 30°$ with ("pen") and without penetration ("not pen") of the surface, and of all scattered H-atoms, for forward scattering ($\phi_f = 0°$).

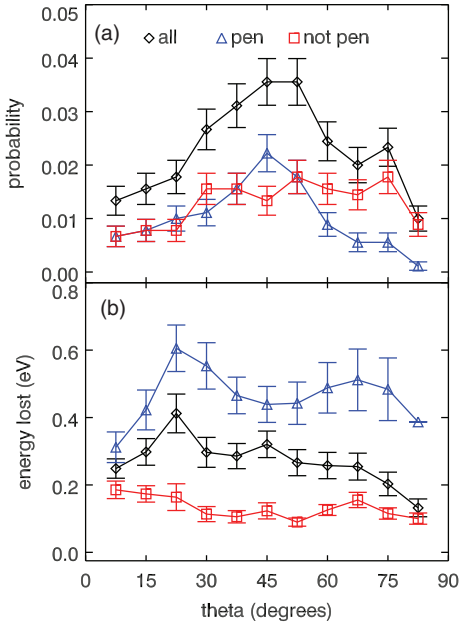

FIG. 9. Angular[19] and energy loss distribution of H-atoms scattering from Au(111) at incidence angles $\theta_i = 15°$ and $\phi_i = 30°$, with ("pen") and without penetration ("not pen") of the surface, and of all scattered H-atoms, for forward scattering ($\phi_f = 0°$).

this incidence condition, Fig. 7(a)). As for Cu (Fig. 7(b)), the angularly resolved ΔE distribution (Fig. 9(b)) suggests that for the model Au(111) surface it should be possible to resolve the contributions of atoms that scatter to these angles with and without penetration by measuring their final translational energy. The atoms scattering to this solid angle region with penetration indeed lose much more energy (Fig. 10(a)).

For the other incidence direction ($\theta_i = 60°$ and $\phi_i = 0°$), we found several solid angle regions to which no atoms scatter with penetration (see Fig. 11(a), for out of plane scattering with $\theta_f = 52.5°$ and $\phi_f = 120°$, and also Figure 3 of Ref. 19 for out of plane scattering with $\theta_f = 60°$ and $\phi_f = 90°$). The angularly resolved ΔE distribution (Fig. 11(b)) suggests that the scattering to $\theta_f = 52.5°$ and $\phi_f = 120°$ should be characterized by small ΔE, as born out by the ΔE distribution for this solid angle region (Fig. 10(b)), see also Figure 4 of Ref. 19 for $\theta_f = 60°$ and $\phi_f = 90°$). For comparison with future calculations on H scattering from Cu(111) or the model Au(111) surface, the present AIMD results regarding solid angle regions to which no or few H-atoms scatter with penetration may not be so reliable as we may have analyzed only a small fraction of the H-atoms that scatter with penetration (Sec. III A). Additionally, our specific prediction for experiments on H + Au(111) will only work if the surface reconstruction of Au(111) has no major effect on the angular distribution of scattering with penetration. But our result suggesting that scattering conditions can be found at which atoms scatter only or predominantly without penetration to specific solid angle regions may also be applicable to H + Ag(111), for which we found the PES to be remarkably similar to the PES for H interacting with the model Au(111) surface (not shown).

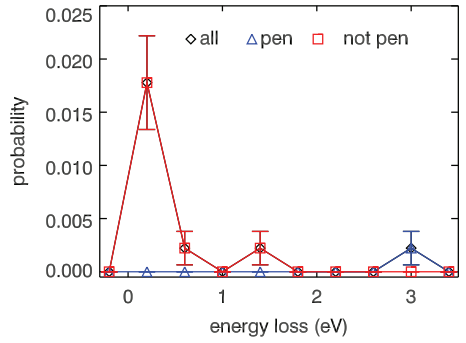

FIG. 8. Energy distribution of H-atoms scattering from Cu(111) for $\theta_i = 15°$ and $\phi_i = 30°$ with ("pen") and without penetration ("not pen") of the surface, and of all scattered H-atoms, for forward scattering ($\phi_f = 0°$) with $\theta_f = 75°$.

For H + Cu(111), we have also found a solid angle region to which scattering occurs exclusively with penetration, in backward scattering with $\theta_f = 22.5°$ (Fig. 12(a)). This result is probably reliable, as we have analyzed more than 90% of the atoms that scatter from the surface without penetration. The atoms that scatter to this solid angle should do so with high $\langle \Delta E \rangle$, although the angularly resolved ΔE distribution does not show a peak for this final solid angle ($\theta_f = 22.5°$, Fig. 12(b)). The relevant final solid angle is close to the incidence angle ($\theta_i = 15.0°$) and it may be hard or even impossible to place the detector in a way so as not to interfere with the incident beam. With the angular resolution used for the scattering angles ($\Delta\phi_f = 60°$ and $\Delta\theta_f = 15°$), for H + Au(111) we have not been able to identify a solid angle region to which scattering occurs exclusively with penetration for either of the two incidence conditions investigated.

Figure 13(a) shows the angular distribution for forward scattering of H from Au(111) for $\theta_i = 60°$ and $\phi_i = 0°$. It shows a maximum for specular scattering (with $\theta_f = \theta_i = 60°$), in contrast to the angular distributions for $\theta_i = 15°$

This article is copyrighted as indicated in the article. Reuse of AIP content is subject to the terms at: http://scitation.aip.org/termsconditions. Downloaded to IP: 134.76.223.157 On: Thu, 18 Sep 2014 11:16:10

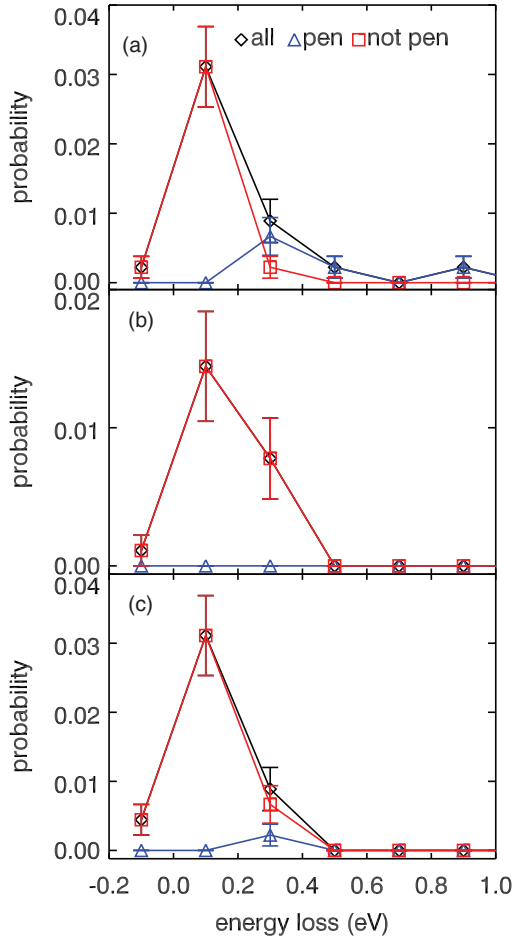

FIG. 10. Energy distribution of H-atoms scattering from Au(111), at incidence angles $\theta_i = 15°$ and $\phi_i = 30°$, for forward scattering ($\phi_f = 0°$) with $\theta_f = 75°$ (a), at incidence angles $\theta_i = 60°$ and $\phi_i = 0°$, for out-of-plane scattering ($\phi_f = 120°$) with $\theta_f = 52.5°$ (b), and for forward scattering ($\phi_f = 0°$) with $\theta_f = 60.0°$ (c). Results are shown for scattering with ("pen") and without penetration ("not pen") of the surface and for scattering of all scattered H-atoms ("all"). The data in panel (c) are taken from Ref. 19.

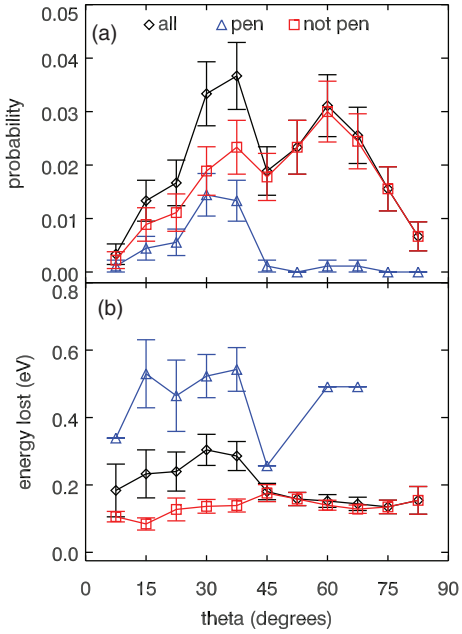

FIG. 11. Angular and energy loss distribution of H-atoms scattering from Au(111) at incidence angles $\theta_i = 60°$ and $\phi_i = 0°$, with ("pen") and without penetration ("not pen") of the surface, and of all scattered H-atoms, for out-of-plane scattering ($\phi_f = 120°$).

and $\phi_i = 30°$ for both Au and Cu (Figs. 9(a) and 7(a)), which peak near 50° and at 30°, respectively. For Au(111) and $\theta_i = 60°$ and $\phi_i = 0°$, the angular distribution for forward in-plane scattering also shows polar angles to which little penetrative scattering occurs, for instance, the specular angle ($\theta_f = 60.0°$ (Fig. 13(a)). The angularly resolved ΔE distribution (Fig. 13(b)) again suggests that for the model Au(111) surface it should be possible to resolve the contributions of atoms that scatter to these angles with and without penetration by measuring their final translational energy. In this case, the contributions from scattering with and without penetration are not completely resolved, but the scattering with penetration only makes a small contribution to the angularly resolved ΔE spectrum (Fig. 10(c)).

We have already noted that scattering to angles ϕ_f and $-\phi_f$ may be different for incidence conditions with $\phi_i = 0°$, as was investigated for H + Au(111). This raises the question of how different angular distributions really are for ϕ_f and $-\phi_f$, the question being of special interest as plots of the H-Au(111) PES suggest that differences should really only result from the incident H-atoms probing the subsurface layers (see Fig. 2). To answer this question, we have performed statistical tests of the null hypothesis that the polar angle scattering distributions with ϕ_f and $-\phi_f$ are the same, which amounts to making the opposite assumption (see Sec. II E). Our results show that the null hypothesis may be rejected with p-values less than 10% for $\phi_f = 90°$ and 120°, less than 5% for $\phi_f = 60°$, and less than 1% for $\phi_f = 30°$ and the case where

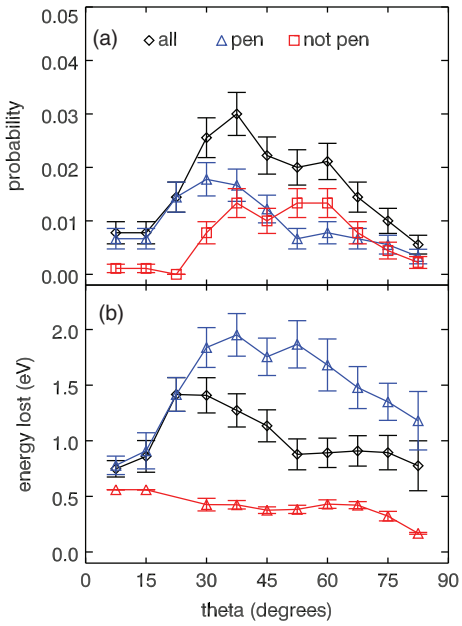

FIG. 12. Angular and energy distribution of H-atoms scattering from Cu(111) for $\theta_i = 15°$ and $\phi_i = 30°$ with ("pen") and without penetration ("not pen") of the surface, and of all scattered H-atoms, for backward scattering ($\phi_f = 180°$).

This article is copyrighted as indicated in the article. Reuse of AIP content is subject to the terms at: http://scitation.aip.org/termsconditions. Downloaded to IP: 134.76.223.157 On: Thu, 18 Sep 2014 11:16:10

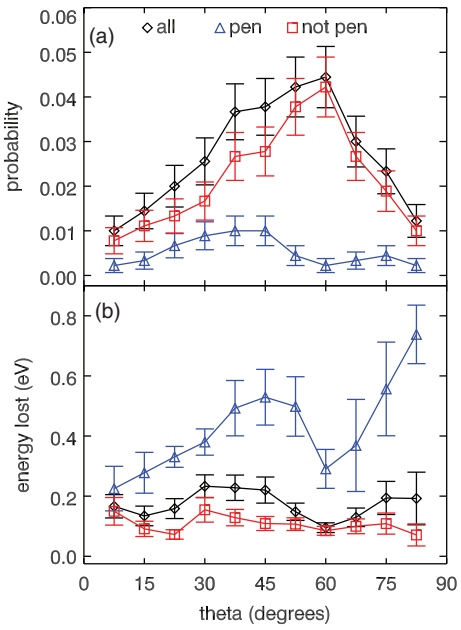

FIG. 13. Angular[19] and energy loss distribution of H-atoms scattering from Au(111) at incidence angles $\theta_i = 60^\circ$ and $\phi_i = 0^\circ$, with ("pen") and without penetration ("not pen") of the surface, and of all scattered H-atoms, for forward scattering ($\phi_f = 0^\circ$).

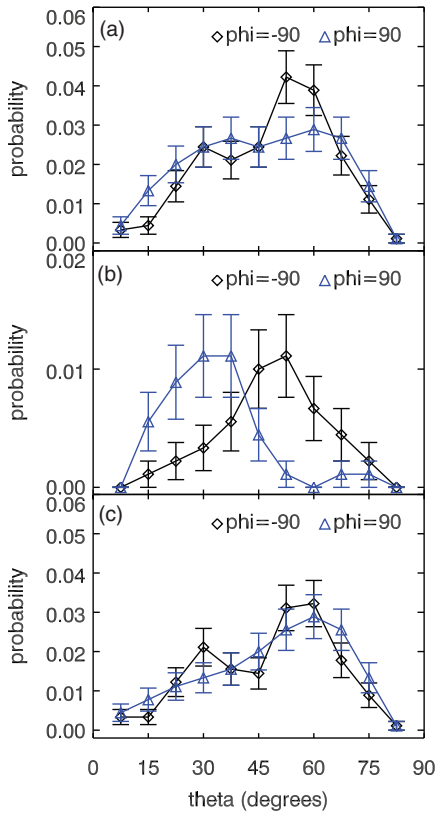

FIG. 14. Angular distribution of H-atoms scattering from Au(111) at incidence angles $\theta_i = 60^\circ$ and $\phi_i = 0^\circ$, are presented for scattering with $\phi_f = 90^\circ$ and -90°, for (a) all trajectories, (b) penetrating trajectories, and (c) non-penetrating trajectories.

data are considered for all ϕ_f (Table III). Angular distributions for scattering with $\phi_f = 90^\circ$ and -90° are compared in Fig. 14. The differences in the distributions of all scattered atoms (Fig. 14(a)) are clearly due to differing distributions of the atoms that scatter with penetration (Fig. 14(b)), showing that the differences arise from atoms probing the subsurface. The results suggest that scattering of hyperthermal H-atoms may be used to probe the crystal structure of the subsurface region of metal surfaces.

D. Non-adiabatic energy loss

The integral non-adiabatic energy loss (ΔE_{NA}) distribution, which includes loss to phonons and to ehp excitation, is shown in Figs. 3(d)–3(f) for H + Cu(111) and for H + Au(111) for the two incidence conditions investigated. The ΔE_{NA} distributions are much wider than the ΔE distribution (Figs. 3(a)–3(c)). For instance, for H + Cu(111), in the non-adiabatic picture the atoms that scatter without penetration on average lose 1.32 eV to the surface, vs. 0.38 eV in the adiabatic picture, and the atoms that scatter with penetration on average lose 3.75 eV to the surface, vs. 1.41 eV in the adiabatic picture (Table I). The $\langle \Delta E_{NA} \rangle$ of all H-atoms scattered from Cu(111) is 2.49 eV, whereas $\langle \Delta E \rangle = 0.88$ eV (Table I). Similar large differences are found for H + Au(111) for both incidence conditions. As already discussed in Sec. III B for $\langle \Delta E \rangle$, the AIMDEFp value of $\langle \Delta E_{NA} \rangle$ of the atoms scattered with penetration is probably underestimated, and the $\langle \Delta E_{NA} \rangle$ of all scattered atoms should likewise be underestimated. The result for $\langle \Delta E_{NA} \rangle$ of the atoms scattered without penetration of the surface has a greater claim to accuracy, as we have analyzed >90% of the relevant trajectories for all systems investigated. A point to note for H + Au(111) for both incidence conditions is that, as penetration of the surface is not involved, the $\langle \Delta E_{NA} \rangle$ value of the H-atoms that scatter from the model Au(111) surface without penetrating it probably also constitutes a reasonably accurate prediction for the reconstructed Au(111) surfaces that can be probed in experiments.

Inspection of Fig. 3(d) further shows that, in the non-adiabatic picture, all H-atoms that scattered with penetration from the Cu(111) surface lost at least 1.4 eV of energy to the surface. All atoms that lose less energy to the surface than 1.4 eV have scattered without penetrating the Cu(111) surface. Likewise, in the non-adiabatic picture all H-atoms scattering with penetration from Au(111) lost at least 1.2 eV of energy for $\theta_i = 15^\circ$ and $\phi_i = 30^\circ$, and at least 1.7 eV of energy for $\theta_i = 60^\circ$ and $\phi_i = 0^\circ$. This suggests a way of distinguishing

TABLE III. For H + Au(111) and $\theta_i = 60^\circ$ and $\phi_i = 0^\circ$, Pearson χ^2 values and p-values for rejecting the null hypothesis that the angular distributions for scattering to $-\phi_f$ are the same as for scattering to $+\phi_f$ are presented. Furthermore, ν is the number of degrees of freedom of the test of the null hypothesis (see Sec. II E).

ϕ_f	χ^2	ν	p-value
150	3.12	6	0.793
120	11.54	6	0.073
90	11.52	6	0.074
60	13.52	6	0.036
30	24.38	6	0.0004
<0	39.25	18	0.0026

This article is copyrighted as indicated in the article. Reuse of AIP content is subject to the terms at: http://scitation.aip.org/termsconditions. Downloaded to IP: 134.76.223.157 On: Thu, 18 Sep 2014 11:16:10

atoms that scatter without and with penetration, if the non-adiabatic picture holds.

In the present non-adiabatic AIMDEFp results, the ΔE_{NA} is calculated without taking into account that the energy dissipation to ehps should slow down the incident H-atoms in the actual trajectories (Sec. II D). Because the instantaneous non-adiabatic energy loss is proportional to the square of the H-atom velocity (Eq. (1)), it may be anticipated that making this approximation leads to an overestimation of the ΔE_{NA}. To verify this, for H + Au(111) and $\theta_i = 15^\circ$, $\phi_i = 30^\circ$ we have done a limited number of AIMDEF calculations in which the friction force acts simultaneously with the DFT adiabatic force,[20] so that the energy dissipation to ehps can slow down the incident H-atoms. In total, 22 AIMDEF trajectories were computed in which scattering occurred without penetration. In these AIMDEF trajectories, as in the AIMDEFp calculations the surface atoms were allowed to move, but the friction coefficients were computed assuming the surface to be static, with the Au(111) atoms in their ideal lattice positions. The computed non-adiabatic energy loss to ehps only (ΔE_{NA}^{eh}, which excludes the loss to phonons) was 0.73 ± 0.11 eV in the AIMDEF calculations (N = 22), compared to 0.91 ± 0.04 eV in the AIMDEFp calculations (N = 900). This limited comparison suggests that the approximation of computing the ΔE_{NA} from the completed AIMD trajectories results in an overestimation of the energy loss to ehps by about 20%.

IV. DISCUSSION

A. Adiabatic scattering probabilities

In Table IV probabilities for scattering without penetration are compared for the three combinations of systems (H + Cu(111) or H + Au(111)) and incidence angles ($\theta_i = 15^\circ$ and $\phi_i = 30^\circ$) or ($\theta_i = 60^\circ$ and $\phi_i = 0^\circ$) considered in this work. We provide both the adiabatic lower bound (determined after 120 fs propagation time) and the adiabatic upper bound to the probability of scattering without penetration. Here, the upper bound takes into account that atoms that have not penetrated but still linger above the surface after 120 fs might still return to the gas phase without penetrating the surface. The probability of scattering without penetration of the surface could be calculated with good accuracy, with the finite propagation time (due to the size of the surface unit cell and slab thickness used here) not severely limiting this accuracy (Table IV). This was not true for the probability of scattering with penetration, as sizeable proportions of the incident atoms either remained on or in the slab after 120 fs or flew through the 4-layer slab modeling the noble metal surface (see Sec. III A). As the total scattering probability also includes the probability of scattering with penetration, our calculations are also much less accurate for this quantity. In principle, an incident H-atom can become accommodated to the surface, especially if the incident H-atom penetrates it. That is, the H-atom can become trapped on or in the surface. However, with our finite propagation time and slab thickness we cannot calculate the accommodation probability (or trapping probability) accurately. Specifically, after 120 fs most of the trapped H-atoms had lost only a fraction of their initial kinetic energy (5 eV). Hence there is considerable uncertainty in the computed total scattering probabilities.

As noted in Sec. III, the larger the probability is for non-penetrative scattering, the greater the chance is that experiments will be able to establish the size of non-adiabatic energy loss to ehps. The reason is that in non-penetrative scattering there are less collisions of the H-atoms with the metal atoms, resulting in smaller energy transfer to the phonons. Therefore, the larger the probability of non-penetrative scattering is, the more clearly the ehp contribution to the energy loss will stand out from the phonon background. Table IV then suggests that to establish energy loss to ehp excitation in scattering of H from Au(111) it is better to work with the more glancing incidence condition ($\theta_i = 60^\circ$ and $\phi_i = 0^\circ$) than with ($\theta_i = 15^\circ$ and $\phi_i = 30^\circ$). It is not yet clear whether this is due to the use of a larger value of θ_i or the use of another incidence plane. Hopefully, future calculations can establish this. Our calculations for the Cu(111) and the model Au(111) surface for the similar incidence condition ($\theta_i = 15^\circ$ and $\phi_i = 30^\circ$) also suggest that, for the purpose stated, it is better to work with the heavier metal (Au) than with the lighter metal (Cu).

B. Energy loss to phonons

For both Cu(111) and for the model Au(111) surface, the average adiabatic energy loss $\langle \Delta E \rangle$ for scattering without penetration (0.38 eV, 0.13 eV, and 0.14 eV for Cu(111), and Au(111) with ($\theta_i = 15^\circ$ and $\phi_i = 30^\circ$) and ($\theta_i = 60^\circ$ and $\phi_i = 0^\circ$), respectively) falls between the values computed for energy loss of H scattering from a single stationary Cu or Au atom with the Baule[42,97] and improved Baule models,[98] respectively (see Tables IV and V). The same is true for the $\langle \Delta E \rangle$ for direct scattering without penetration (see Tables I, IV, and V). In the collinear hard sphere Baule model, the energy ΔE transferred by the projectile atom with mass m_a and kinetic energy E_i to the target atom with mass m_s is given by[42,97]

$$\Delta E = \frac{4\mu E_i}{(1+\mu)^2}, \tag{3}$$

where the mass ratio $\mu = m_a/m_s$. In the improved Baule model, the well depth ε of the molecule-surface interaction (see Table V and Sec. II B) is added to E_i to describe the effect of the pre-acceleration of the atom in the potential well.[98] The good comparison of the actual computed energy losses of H-atoms scattering non-penetratively from Cu(111) and Au(111) to the Baule model values suggests that, from an energy transfer point of view, in the adiabatic picture the non-penetrative scattering is well described by a simple model. In this model the H atom scatters from a single surface atom, which does not "feel" the surrounding of the other metal atoms. This implies that the surface reconstruction of Au(111) will not much affect energy losses in non-penetrative scattering of H-atoms, so that it should be possible to obtain accurate energy losses for this system with the model Au(111) surface used here. It also implies that the non-penetrative scattering of hyperthermal H-atoms from Cu(111) and Au(111) occurs in the regime of structure scattering, where the energy

This article is copyrighted as indicated in the article. Reuse of AIP content is subject to the terms at: http://scitation.aip.org/termsconditions. Downloaded to IP: 134.76.223.157 On: Thu, 18 Sep 2014 11:16:10

TABLE IV. Probabilities (p), adiabatic energy losses (ΔE) calculated with AIMD, and non-adiabatic energy losses (ΔE_{NA}) calculated with AIMDEFp are provided for scattering without penetration and for scattering, for the three combinations of system and incidence angles considered here, for $E_i = 5$ eV. Also shown is the energy ΔE^{peak} at which the low energy peak occurs in the adiabatic energy loss spectrum, and the energy ΔE_{NA}^{peak} at which the lowest energy peak occurs in the non-adiabatic energy loss spectrum. Energy losses are expressed in eV. Part of the data contained in the table have been published earlier in Ref. 19.

Observable	H + Cu(111) $\theta_i = 15°$, $\phi_i = 30°$	H + Au(111) $\theta_i = 15°$, $\phi_i = 30°$	H + Au(111) $\theta_i = 60°$, $\phi_i = 0°$
p, scattering without penetration	0.30–0.33	0.38–0.40	0.58–0.64
ΔE, scattering without penetration	0.38	0.13	0.14
ΔE_{NA}, scattering without penetration	1.32	1.04	1.14
p, scattering	0.58–1.0	0.66–1.0	0.72–1.0
ΔE, scattering	0.88	0.29	0.21
ΔE^{peak}	0.325	0.1125	0.1125
ΔE_{NA}^{peak}	0.575	0.3265	0.4125
ΔE_{NA}, scattering	2.49	1.93	1.52

of the incoming atom is so high that the atom-surface potential is dominated by the interaction with single surface atoms.[99]

Looking at the integral energy loss spectra (Figs. 3(a)–3(c)), we see that the electronically adiabatic model predicts that the spectra should contain a well-resolved low energy peak, and a structured tail towards higher ΔE. For all three combinations of system and incidence condition, the low energy feature peaks at an energy, ΔE^{peak}(325 meV, 112.5 meV, and 112.5 meV, respectively (Table IV), for Cu(111), Au(111) and ($\theta_i = 15°$ and $\phi_i = 30°$), Au(111) and ($\theta_i = 60°$ and $\phi_i = 0°$)), which falls within the range of values predicted by the simple and improved Baule model (305-450 meV for Cu and 101-140 meV for Au). Extrapolating to the Ag(111) surface, we would predict that, for the combinations of incidence angles investigated and $E_i = 5$ eV, the adiabatic energy loss spectrum would have a similar appearance to the energy loss spectra shown in Figs. 3(a)–3(c), but that the low energy peak would occur between 182 and 253 meV (see Table V). We would also predict that the $\langle \Delta E \rangle$ of H-atoms scattering from the Ag(111) surface without penetration would fall between these two values. In the adiabatic picture, the integral energy loss spectra show ΔE^{peak} values that are 20% lower than the computed $\langle \Delta E \rangle$ of H-atoms scattering without penetration. This suggests that, if the adiabatic picture applies, measured values of ΔE^{peak} could be used to arrive at an experimental estimate of the average energy loss of H-atoms scattering without surface penetration.

TABLE V. Potential well depths ε, values of the adiabatic energy loss predicted with the Baule model (ΔE_B) and with the improved Baule model (ΔE_{IB}) are given for Cu, Ag, and Au.

Metal surface	ε (eV)	ΔE_B (eV)	ΔE_{IB} (eV)
Cu(111)	2.37	0.305	0.450
Ag(111)	1.96	0.182	0.253
Au(111)	1.97	0.101	0.140

C. Non-adiabatic energy loss to phonons and ehps

For both Cu(111) and for the model Au(111) surface, and for the latter surface for both incidence conditions, the non-adiabatic energy loss to the surface significantly exceeds the adiabatic energy loss, making ehp excitation the dominant energy loss channel for the systems and conditions addressed. For non-penetrative scattering, $\langle \Delta E_{NA} \rangle$ exceeds $\langle \Delta E \rangle$ by about 0.9-1.0 eV (1.32 vs. 0.38 eV, 1.04 vs. 0.13 eV, and 1.14 vs. 0.14 eV for Cu(111), and Au(111) with ($\theta_i = 15°$ and $\phi_i = 30°$) and ($\theta_i = 60°$ and $\phi_i = 0°$), respectively, see Table IV). Experimentally, the effect of non-adiabatic energy loss to ehps should be clearly visible in shifts of the position of the lowest energy peak (ΔE^{peak}) in the integral energy loss spectrum of 0.2–0.3 eV, from 0.325 to 0.575 eV for Cu(111), from 0.113 to 0.327 eV for Au(111) and ($\theta_i = 15°$ and $\phi_i = 30°$), and from 0.113 to 0.413 eV for Au(111) and ($\theta_i = 60°$ and $\phi_i = 0°$), respectively (see Table IV and Figs. 3). For Au, these shifts (0.2–0.3 eV) are larger than the actual values (about 0.11 eV) of ΔE^{peak} in the adiabatic energy loss spectrum (Table IV). Taking a possible overestimation of the energy transfer to ehps by about 20% into account (due to not taking into account the lowering of the velocity of H due to energy transfer to ehps in the AIMDEFp calculations, see Sec. III D), the effect of the non-adiabaticity should still be clearly visible in the energy loss spectra.

In our discussion of energy loss, for both the adiabatic case (Sec. IV B) and the non-adiabatic case we have not been emphasizing the energy loss suffered by all scattered H-atoms, or the energy loss suffered by H-atoms that scattered with penetration. The reason for this is that in these cases we may have analyzed considerably less than 50% of all the H-atoms that could scatter with surface penetration (see Sec. III). Because we are not taking into account the contribution of H-atoms that could scatter with penetration of 4 or more layers, and of H-atoms that have lingered in the metal slab for longer times than we could simulate, we probably underestimate the energy loss of the atoms that scattered with penetration, and therefore also of all the scattered H-atoms. It

This article is copyrighted as indicated in the article. Reuse of AIP content is subject to the terms at: http://scitation.aip.org/termsconditions. Downloaded to IP: 134.76.223.157 On: Thu, 18 Sep 2014 11:16:10

is nevertheless useful to note that, for all scattering trajectories taken together, the average non-adiabatic energy loss exceeds the average adiabatic energy loss by 1.3-1.6 eV for the combinations of system and incidence conditions studied (see Table IV).

The contributions to the energy loss spectra of the two different categories of H-atoms stand out rather clearly in our calculations. In both the adiabatic and the non-adiabatic calculations the lowest energy peak in the spectra is mostly (exclusively in the non-adiabatic case, Figs. 3(d)–3(f), and almost exclusively in the adiabatic case, Figs. 3(a)–3(c)) due to non-penetrative scattering. Especially for Au(111), the adiabatic and non-adiabatic energy loss spectra look qualitatively different: The adiabatic energy loss spectra consist of one single low energy peak and a "blue" (high-energy) tail which has essentially petered out at an energy loss of 1 eV, whereas the non-adiabatic spectra also show other prominent high energy peaks and a blue tail extending to energy losses >2.0 eV. The qualitative differences in the appearance of the spectra can serve as signatures for the importance of non-adiabatic effects (energy transfer to ehp excitation). We expect this to hold independently of the surface reconstruction of Au(111), as for Au the appearance of the energy loss spectrum for energies less than 1 eV is completely determined by H-atoms that scatter non-penetratively. We expect that the scattering of this category of atoms should not be much affected by the surface reconstruction of Au(111), as also suggested by our observation that the average adiabatic energy loss of these H-atoms is well described by Baule models (see Sec. IV B).

It is also of interest to compare the calculated ratio of the energy losses to ehp excitation and to phonons for non-penetrative scattering of H from Cu(111) (2.5, from the results of Table I) to the analogous ratio of the energy relaxation rates predicted earlier for the same system by Hammer and co-workers.[41] They computed an energy relaxation rate due to phonon excitation of 0.7×10^{12} s^{-1} for H + Cu(111), and their estimate (1.6×10^{12} s^{-1}) of the energy relaxation rate to ehp excitation from observed vibrational line widths of H adsorbed on Cu(111)[31] was larger than the loss rate to phonons by a factor 2.3 (see also Sec. I). This ratio of the energy relaxation rates (2.3) compares well to the ratio we compute for the energy losses to ehp excitation and phonons (2.5). This comparison suggests that (i) vibrational line widths of H adsorbed to a specific metal surface might yield a quantitatively accurate measure of the average strength of *T-ehp coupling* that hyperthermal H-atoms scattering from that same metal surface would experience, and that (ii) the approach of using friction coefficients computed with the LDFA method[10] to model non-adiabatic interactions of hyperthermal H-atoms interacting with metal surfaces like Cu(111) models these interactions with reasonable accuracy. At this point, this conclusion is speculative, as the present finding of similar ratios might be due to error cancellations resulting from differences in the regions of the configuration space sampled and the approach taken to model non-adiabatic interactions. But the finding of similar ratios is intriguing, and we suggest that future work explore whether also for other H-metal surface systems there are similarities between the strength of the *T-ehp coupling* that is experienced by scattered H-atoms and the coupling strength determined from vibrational line width measurements of H adsorbed to the same surface.

D. Angular scattering distributions

Our AIMD calculations predict that scattering of H-atoms from Cu(111) and Au(111) at $E_i = 5$ eV leads to extremely broad angular distributions, in both the forward and backward directions, and in sideways directions as well (Figs. 4–6). Although this is true for both scattering with and without penetration (Figs. 4–6), our calculations nevertheless suggest that, if the adiabatic picture applies, solid angle regions exist to which atoms scatter only with or only without penetration, for the H + Cu(111) case studied and for H + the model Au(111) surface with ($\theta_i = 60^\circ$ and $\phi_i = 0^\circ$). The result regarding the absence of penetrative scattering to specific final solid angles may be somewhat less reliable as we may have analyzed less than 50% of the atoms that scattered with penetration. However, even if a small fraction of atoms would scatter to a specific solid angle with penetration, usually it should be easy to distinguish these atoms in the associated angularly resolved energy loss spectrum, due to their larger energy loss. Solid angles to which no or only few atoms scatter with penetration are of special interest to detecting non-adiabatic energy loss, as this loss should stand out against a small energy loss to phonons of atoms that scattered only or predominantly without penetration. On this point, our predictions for H + Cu(111) (of predominantly non-penetrative scattering for forward scattering with ($\theta_i = 15^\circ$ and $\phi_i = 30^\circ$) incidence angles and $\theta_f = 75^\circ$, see Figs. 7 and 8) should be more reliable than analogous predictions for H + Au(111), because whether or not penetrated atoms scatter to a specific solid angle should depend on whether the surface reconstructs (in experiments on Au(111)) or not (in the present calculations).

Experimentally, it should be much easier to measure energy loss spectra for specific final solid angles than to measure integral energy loss spectra. An advantage of Au over Cu is that it is heavier and therefore less energy loss is incurred to phonons, due to the smaller μ-value for H on Au. This should make it easier to distinguish non-adiabatic contributions to energy loss in integral energy loss distributions for Au(111). On the other hand, predicting solid angle regions to which H-atoms scatter only or predominantly without penetration is hard to do for Au(111), as it requires the simulation of a reconstructed surface, which is currently not doable with AIMD. We suggest that Ag(111) could represent a good compromise here. The μ-value for H on Ag is sufficiently small that little energy transfer is expected to the phonons from application of the Baule models (Table V), which bracket the predicted energy transfer in adiabatic scattering of H from Cu(111) and the model Au(111) surface. Non-adiabatic energy losses should therefore still stand out quite well against adiabatic energy losses for the Ag(111) surface. Because Ag(111) does not reconstruct AIMD calculations should be able to reliably predict solid angle regions to which scattering occurs only or predominantly without penetration. Such calculations should therefore be able to make useful predictions for experiments aimed at detecting

This article is copyrighted as indicated in the article. Reuse of AIP content is subject to the terms at: http://scitation.aip.org/termsconditions. Downloaded to IP: 134.76.223.157 On: Thu, 18 Sep 2014 11:16:10

non-adiabatic energy loss in scattering of H-atoms from metal surfaces.

E. Hyperthermal H-atom scattering as a means of probing the subsurface region

For scattering of H-atoms from the model Au(111) surface at incidence in the $[10\bar{1}]$ direction, the polar angular distributions for scattering to $+\phi_f$ and $-\phi_f$ differ significantly for several values of ϕ_f (see Fig. 14, Table III, and Sec. III C). The differences arise from the contribution of the atoms that scatter penetratively (see Fig. 14 and Sec. III C), which might be expected as the differences between the interaction of H with the fcc and hcp sites (and between the t2f and t2h sites) become pronounced only below the surface (Fig. 2). These results show that adiabatic scattering of hyperthermal atoms with $E_i = 5$ eV from the model Au(111) surface is sensitive to the structure of the subsurface region of Au(111). Adiabatic calculations for incidence along the $[10\bar{1}]$ direction have not been done for Cu(111) and Ag(111), but we expect that a similar result should hold for these surfaces. What is not yet clear is how large the effect of the subsurface will be for these surfaces, and whether non-adiabatic effects will weaken or reinforce the effects of the subsurface.

The fact that 5 eV H-atoms can probe the subsurface region of a metal surface may be of interest to the field of surface analysis. Alternative methods for probing this region exist, such as Medium Energy Ion Scattering and Low Energy Electron Diffraction (MEIS and LEED, see also Ref. 100) but these techniques may be more disruptive to the surface, involving charged particles at higher E_i (20-500 eV for LEED, 100 keV for MEIS).

F. Directions for future research

Our research suggests a number of directions for future research, which can be grouped in exploring non-adiabatic effects, using more approximate models for the molecule-surface interaction to achieve better statistics and enable longer simulation times, the exploration of other incidence conditions and metal surfaces, and suggestions for experiments.

Our AIMDEFp results clearly suggest a large effect of ehp excitation, which is predicted to be the predominant source of energy loss in scattering of H-atoms from Au(111). On the other hand, the calculations still use a number of approximations that need further testing. For non-penetrative scattering of H from Au(111) the approximation used in AIMDEFp of evaluating energy loss based on AIMD trajectories (i.e., not correcting the instantaneous H velocity for energy dissipation to ehps) leads to an overestimation of the energy transferred to ehps by about 20% (see Sec. III D). This number is currently based on a limited number of AIMDEF trajectories (only 22), and additional AIMDEF calculations could be done to obtain more accurate and more definite numbers. These calculations could also test another approximation made, of basing the friction coefficients on the electron density of the ideal, static metal surface. This approximation probably has a small effect on the evaluated energy loss, as we do not expect considerable changes in the electron densities probed by the H-atom as a consequence of surface atom displacements. Nevertheless, the size of this effect is unclear, and calculations should be done to address this.

As also pointed out in Sec. II D, different methods for evaluating friction coefficients exist (for instance, the LDFA method used here[10] and the method used by Trail *et al.*,[40] which are compared in Ref. 19). Non-adiabatic effects in scattering of H from metal surfaces have also been studied with different approaches, which also describe non-adiabatic effects due to the quenching of the spin of H.[7,101,102] It would be worthwhile to perform AIMDEF calculations with friction coefficients based on different methods, and also to perform TDDFT-MD calculations (combining Ehrenfest dynamics for the nuclei with time-dependent DFT for the electrons[7]) to explore to what extent these methods yield differing results. We suggest that such calculations will be most profitable once the experiments discussed in the Introduction become available. Our result that non-adiabatic effects are likely to be large suggests that the experiments can be used to assess the accuracy of methods for computing friction coefficients, or, more generally, of non-adiabatic methods.

AIMD calculations are computationally expensive and for this reason only a restricted number of trajectories could be calculated. This has the disadvantage that the statistical accuracy of the calculations is rather low. The statistical accuracy can be improved by using potential models instead of AIMD, as calculations using such models are computationally much less expensive. Examples of potential models that could be used include effective medium theory (EMT),[103–105] which has been used already in explorative calculations on H + Au(111)[70] and in calculations on H + Cu(111),[41] and potentials based on neural networks.[106,107] It would be worthwhile to explore whether such calculations could model scattering of H atoms from reconstructed Au(111). Furthermore, with MD simulations collisions can be simulated for much longer times than was possible here, and this should also allow the calculation of probabilities of H getting trapped on or in the surface. A point of attention with the potentials models that have to be used with MD is of course whether they faithfully represent the interaction of H with the metal surface. The AIMD results presented here can serve as useful benchmarks for MD and molecular dynamics with electronic friction (MDEF) calculations testing such potential models.

Our calculations have so far only explored a limited number of incidence conditions (only one E_i (5 eV), one T_s (120 K), two combinations of incidence angles, and two metal surfaces). It would be worthwhile to explore combinations of ranges of E_i, T_s, and incidence angles (θ_i and ϕ_i) accessible in experiments. In view of the high computational expense of AIMD, this is perhaps best done using potential models. As already pointed out in Sec. IV D, it may also be worthwhile to perform calculations on H + Ag(111), as non-adiabatic effects would still be expected to dominate the energy loss for this system while the Ag(111) surface does not reconstruct, in contrast to the Au(111) surface.

The present work contains some obvious suggestions for experiments. If possible, integral energy loss spectra should

This article is copyrighted as indicated in the article. Reuse of AIP content is subject to the terms at: http://scitation.aip.org/termsconditions. Downloaded to IP: 134.76.223.157 On: Thu, 18 Sep 2014 11:16:10

be determined. Measurement of ΔE^{peak} in the energy loss spectrum will show whether the energy loss is dominated by the phonons (energy loss bracketed by Baule model and improved Baule model) or whether loss to ehps is important or even predominates. This should work for H + Cu(111), but also for H + Au(111), even though our simulations are for the model Au(111) surface, because the peak position referred to is determined by non-penetrative scattering. As discussed above, H + Ag(111) might be the best system to explore, as Ag(111) does not reconstruct so that experiments on this system would make for a more straightforward interaction with theory. For instance, we suggest that experiments be done on H + Ag(111) to explore whether hyperthermal H atoms can be used to explore the subsurface region of the surface, with a technique that in principle should be less invasive than other surface analysis techniques that could be used for this purpose, such as MEIS and LEED.

V. CONCLUSIONS AND OUTLOOK

This paper presents results of AIMD calculations on scattering of H from Cu(111) and from a model Au(111) surface, for $E_i = 5$ eV, $T_s = 120$ K, and for one combination of incidence angles for Cu and two combinations of incidence angles for Au. The calculations have been done with the SRP48 density functional, which previously gave a chemically accurate description of a number of experiments on reactive scattering of H_2 from Cu(111). We have also used the AIMD trajectories to predict non-adiabatic energy losses to ehp excitation, in AIMDEFp calculations based on the LDFA. Our results may be viewed as predictions for experiments that can be done using photodissociation of HCl or HBr to make velocity selected beams of H, and Rydberg tagging with time-of-flight techniques to measure the H-atoms scattered from the surface in an energy resolved way. A caveat for Au is that the predictions are made for the model ideal Au(111) surface, while in reality Au(111) is known to reconstruct. The conclusions from the calculations are as follows:

1. With our current AIMD model and implementation, accurate predictions can be made for the probability that H scatters from the metal surface without penetrating it, under the assumption of electronic adiabaticity.
2. The probability of scattering without penetration is greater for the model Au(111) surface than for Cu(111), and for Au(111) greater for ($\theta_i = 60^\circ$ and $\phi_i = 0^\circ$) than for ($\theta_i = 15^\circ$ and $\phi_i = 30^\circ$).
3. For Cu(111) and the model Au(111) surface, the AIMD calculations predict an average energy loss to the phonons of 0.38 eV and 0.13-0.14 eV, respectively, for non-penetrative scattering. The fact that these values closely correspond to energy losses predicted with Baule models suggests that in non-penetrative scattering from Cu(111) and Au(111) H scatters from a single surface atom ("structure scattering"), which is essentially independent of the metal surface environment from an energy transfer viewpoint. It also suggests that our results for energy losses in non-penetrative scattering from the model Au(111) surface represent accurate predictions for the experimentally realizable reconstructed Au(111) surface.
4. In the adiabatic picture, the predicted integral energy loss spectra all display a lowest energy peak at an energy corresponding to 80% of the average adiabatic energy loss in non-penetrative scattering. This peak is due to non-penetrative scattering. The predicted ΔE^{peak} only slightly exceed the energy losses predicted with the simple Baule model. In the non-adiabatic picture these peaks are shifted to higher energy losses by 0.2-0.3 eV. On the basis of these predictions, we suggest experiments to measure the position of the peak referred to in the integral energy loss spectrum to determine the relative importance of energy loss to ehps. Our results for the model Au(111) surface should also be reliable for reconstructed Au(111), as the peak position referred to is due to non-penetrative scattering. The comparison of our AIMD with AIMDEFp results predicts that non-adiabatic effects in energy loss in scattering from Au(111) should be easy to detect for this system. In view of the predictive power of the simple Baule model for phonon inelastic scattering and the size of the non-adiabatic energy losses found for Cu and Au, we predict that the same should hold for experiments on H + Ag(111).
5. The average non-adiabatic energy losses for non-penetrative scattering of H from Cu(111) and Au(111) exceed the adiabatic energy losses (to phonons only) by 0.9-1.0 eV. Ehp excitation therefore constitutes the dominant energy dissipation channel for the scattering conditions and metal surfaces addressed here. In view of the large predicted non-adiabatic effects on energy losses, scattering experiments measuring such energy losses could provide useful benchmarks for theoretical methods for evaluating friction coefficients, which can then be tested by comparison of AIMDEF calculations with the said experiments.
6. The adiabatic and non-adiabatic integral energy loss spectra have qualitatively different appearances. In the non-adiabatic spectra the lowest energy peak is far less prominent, and the spectra contain far broader tails extending to much larger values of the energy loss.
7. The AIMD calculations predict that scattering of H atoms from Cu(111) and Au(111) under the conditions investigated leads to extremely broad angular distributions. For H + Cu(111), for $E_i = 5$ eV, $T_s = 120$ K, and for ($\theta_i = 15^\circ$ and $\phi_i = 30^\circ$), our AIMD calculations predict that scattering with ($\theta_f = 75^\circ$ and $\phi_f = 0^\circ$) should predominantly occur without penetration. The measurement of an energy loss spectrum similar to that shown in Fig. 8, which predominantly shows small energy losses characteristic of energy transfer to phonons, would constitute strong proof that non-adiabatic effects are not important. On the other hand, the measurement of far greater energy losses under these conditions would constitute proof of the importance of ehp excitation.
8. Our AIMD results for incidence of H on the model Au(111) surface along the $[10\bar{1}]$ direction suggest that

This article is copyrighted as indicated in the article. Reuse of AIP content is subject to the terms at: http://scitation.aip.org/termsconditions. Downloaded to IP: 134.76.223.157 On: Thu, 18 Sep 2014 11:16:10

hyperthermal beams of H-atoms may be used to probe the subsurface regions of metal surfaces like Cu(111) and Ag(111).

We suggest the following directions for future theoretical research:

1. AIMDEF calculations could be done to investigate the effects of the approximations made in the present AIMDEFp calculations, and of the model used to compute friction coefficients, on the non-adiabatic energy losses we predicted in our three model studies.
2. MD and MDEF calculations employing accurate potential models can be done to achieve results with greater statistical accuracy and based on longer simulation times, and to explore a greater range of incidence conditions and metal surfaces. The reliability of potential models can be benchmarked on our AIMD results for Cu(111) and the model Au(111) surface.
3. New calculations and experiments on H + Ag(111) could be of special interest, this system representing a good compromise between dominance of non-adiabatic effects over phonon-effects (for which Au would be even better) and the degree to which the surface can be prepared in a well-defined manner (Ag(111) enjoying the advantage that it does not reconstruct, as opposed to Au(111)).

ACKNOWLEDGMENTS

We thank J. I. Juaristi, A. M. Wodtke, A. Kandratsenka, and S. M. Janke for useful discussions. We thank the Stichting Nationale Computerfaciliteiten (NCF) for grants of computing time. D.J.A. is grateful for support from the Leiden Institute of Chemistry as a van Arkel visiting professor, and for support of the Alexander von Humboldt Foundation. M.B.-R. acknowledges financial support from the European Commission through Project No. FP7-PEOPLE-2010-RG276921. M.A. acknowledges the Gobierno Vasco-UPV/EHU Project IT-756-13 and the Spanish MICINN Project FIS2010-19609-C02-02.

[1] Y. H. Huang, C. T. Rettner, D. J. Auerbach, and A. M. Wodtke, Science **290**, 111 (2000).
[2] Y. Huang, A. M. Wodtke, H. Hou, C. T. Rettner, and D. J. Auerbach, Phys. Rev. Lett. **84**, 2985 (2000).
[3] B. Gergen, H. Nienhaus, W. H. Weinberg, and E. W. McFarland, Science **294**, 2521 (2001).
[4] A. J. Komrowski, J. Z. Sexton, A. C. Kummel, M. Binetti, O. Weisse, and E. Hasselbrink, Phys. Rev. Lett. **87**, 246103 (2001).
[5] J. D. White, J. Chen, D. Matsiev, D. J. Auerbach, and A. M. Wodtke, Nature **433**, 503 (2005).
[6] P. Nieto, E. Pijper, D. Barredo, G. Laurent, R. A. Olsen, E. J. Baerends, G. J. Kroes, and D. Farías, Science **312**, 86 (2006).
[7] M. Lindenblatt and E. Pehlke, Phys. Rev. Lett. **97**, 216101 (2006).
[8] Q. Ran, D. Matsiev, D. J. Auerbach, and A. M. Wodtke, Phys. Rev. Lett. **98**, 237601 (2007).
[9] G. J. Kroes, Science **321**, 794 (2008).
[10] J. I. Juaristi, M. Alducin, R. Díez Muiño, H. F. Busnengo, and A. Salin, Phys. Rev. Lett. **100**, 116102 (2008).
[11] N. H. Nahler, J. D. White, J. Larue, D. J. Auerbach, and A. M. Wodtke, Science **321**, 1191 (2008).
[12] A. C. Luntz, I. Makkonen, M. Persson, S. Holloway, D. M. Bird, and M. S. Mizielinski, Phys. Rev. Lett. **102**, 109601 (2009).
[13] J. I. Juaristi, M. Alducin, R. Díez Muiño, H. F. Busnengo, and A. Salin, Phys. Rev. Lett. **102**, 109602 (2009).
[14] N. Shenvi, S. Roy, and J. C. Tully, Science **326**, 829 (2009).
[15] X. Z. Ji, A. Zuppero, J. M. Gidwani, and G. A. Somorjai, J. Am. Chem. Soc. **127**, 5792 (2005).
[16] C. Bartels, R. Cooper, D. J. Auerbach, and A. M. Wodtke, Chem. Sci. **2**, 1647 (2011).
[17] E. Hasselbrink, Science **326**, 809 (2009).
[18] L. Martin-Gondre, M. Alducin, G. A. Bocan, R. Díez Muiño, and J. I. Juaristi, Phys. Rev. Lett. **108**, 096101 (2012).
[19] M. Pavanello, D. J. Auerbach, A. M. Wodtke, M. Blanco-Rey, M. Alducin, and G. J. Kroes, J. Phys. Chem. Lett. **4**, 3735 (2013).
[20] M. Blanco-Rey, J. I. Juaristi, R. Díez Muiño, H. F. Busnengo, G. J. Kroes, and M. Alducin, Phys. Rev. Lett. **112**, 103203 (2014).
[21] J. R. Trail, M. C. Graham, D. M. Bird, M. Persson, and S. Holloway, Phys. Rev. Lett. **88**, 166802 (2002).
[22] S. N. Maximoff and M. P. Head-Gordon, Proc. Natl. Acad. Sci. U.S.A. **106**, 11460 (2009).
[23] J. Y. Park, J. R. Renzas, A. M. Contreras, and G. A. Somorjai, Top. Catal. **46**, 217 (2007).
[24] G. A. Somorjai, and J. Y. Park, J. Chem. Phys. **128**, 182504 (2008).
[25] K. Schönhammer and O. Gunnarsson, Surf. Sci. **117**, 53 (1982).
[26] C. Díaz, E. Pijper, R. A. Olsen, H. F. Busnengo, D. J. Auerbach, and G. J. Kroes, Science **326**, 832 (2009).
[27] N. Shenvi, S. Roy, and J. C. Tully, J. Chem. Phys. **130**, 174107 (2009).
[28] A. M. Wodtke, D. Matsiev, and D. J. Auerbach, Prog. Surf. Sci. **83**, 167 (2008).
[29] C. T. Rettner, F. Fabre, J. Kimman, and D. J. Auerbach, Phys. Rev. Lett. **55**, 1904 (1985).
[30] M. Grotemeyer and E. Pehlke, Phys. Rev. Lett. **112**, 043201 (2014).
[31] C. L. A. Lamont, B. N. J. Persson, and G. P. Williams, Chem. Phys. Lett. **243**, 429 (1995).
[32] J. E. Reutt, Y. J. Chabal, and S. B. Christman, Phys. Rev. B **38**, 3112 (1988).
[33] H. Nienhaus, Surf. Sci. Rep. **45**, 1 (2002).
[34] J. T. Kindt, J. C. Tully, M. Head-Gordon, and M. A. Gomez, J. Chem. Phys. **109**, 3629 (1998).
[35] J. Meyer and K. Reuter, New J. Phys. **13**, 085010 (2011).
[36] U. Bischler, P. Sandl, E. Bertel, T. Brunner, and W. Brenig, Phys. Rev. Lett. **70**, 3603 (1993).
[37] J. K. Nørskov and B. I. Lundqvist, Surf. Sci. **89**, 251 (1979).
[38] G. P. Brivio and T. B. Grimley, Surf. Sci. **161**, L573 (1985).
[39] G. P. Brivio, T. B. Grimley, and A. Devescovi, J. Electron Spectrosc. Relat. Phenom. **45**, 391 (1987).
[40] J. R. Trail, D. M. Bird, M. Persson, and S. Holloway, J. Chem. Phys. **119**, 4539 (2003).
[41] J. Strömquist, L. Bengtsson, M. Persson, and B. Hammer, Surf. Sci. **397**, 382 (1998).
[42] A. Gross, *Theoretical Surface Science: A Microscopic Perspective* (Springer, Berlin, 2003).
[43] O. Buenermann and A. M. Wodtke, private communication (2013).
[44] L. Schnieder, K. Seekamp-Rahn, E. Wrede, and K. H. Welge, J. Chem. Phys. **107**, 6175 (1997).
[45] X. M. Yang, Int. Rev. Phys. Chem. **24**, 37 (2005).
[46] H. A. Michelsen, C. T. Rettner, D. J. Auerbach, and R. N. Zare, J. Chem. Phys. **98**, 8294 (1993).
[47] C. T. Rettner, H. A. Michelsen, and D. J. Auerbach, J. Chem. Phys. **102**, 4625 (1995).
[48] J. Dai and J. C. Light, J. Chem. Phys. **107**, 1676 (1997).
[49] F. Nattino, C. Díaz, B. Jackson, and G. J. Kroes, Phys. Rev. Lett. **108**, 236104 (2012).
[50] C. T. Rettner and D. J. Auerbach, J. Chem. Phys. **104**, 2732 (1996).
[51] T. Kammler and J. Küppers, J. Chem. Phys. **111**, 8115 (1999).
[52] C. D. Vurdu and Z. B. Güvenç, J. Chem. Phys. **134**, 164306 (2011).
[53] D. V. Shalashilin, B. Jackson, and M. Persson, J. Chem. Phys. **110**, 11038 (1999).
[54] S. Caratzoulas, B. Jackson, and M. Persson, J. Chem. Phys. **107**, 6420 (1997).
[55] C. Kalyanaraman, D. Lemoine, and B. Jackson, Phys. Chem. Chem. Phys. **1**, 1351 (1999).
[56] J. Dai and J. C. Light, J. Chem. Phys. **110**, 6511 (1999).
[57] A. R. Sandy, S. G. J. Mochrie, D. M. Zehner, K. G. Huang, and D. Gibbs, Phys. Rev. B **43**, 4667 (1991).

This article is copyrighted as indicated in the article. Reuse of AIP content is subject to the terms at: http://scitation.aip.org/termsconditions. Downloaded to IP: 134.76.223.157 On: Thu, 18 Sep 2014 11:16:10

[58]U. Harten, A. M. Lahee, J. P. Toennies, and Ch. Wöll, Phys. Rev. Lett. **54**, 2619 (1985).
[59]F. Hanke and J. Björk, Phys. Rev. B **87**, 235422 (2013).
[60]B. Schindler, D. Diesing, and E. Hasselbrink, Z. Phys. Chem. **227**, 1381 (2013).
[61]B. Schindler, D. Diesing, and E. Hasselbrink, J. Chem. Phys. **134**, 034705 (2011).
[62]B. Schindler, D. Diesing, and E. Hasselbrink, J. Phys. Chem. C **117**, 6337 (2013).
[63]H. Nienhaus, H. S. Bergh, B. Gergen, A. Majumdar, W. H. Weinberg, and E. W. McFarland, Phys. Rev. Lett. **82**, 446 (1999).
[64]D. Krix, R. Nünthel, and H. Nienhaus, Phys. Rev. B **75**, 073410 (2007).
[65]D. Krix, R. Nünthel, and H. Nienhaus, J. Vac. Sci. Technol. A **25**, 1156 (2007).
[66]D. A. Kovacs, T. Babkina, T. Gans, U. Czarnetzki, and D. Diesing, J. Phys. D: Appl. Phys. **39**, 5224 (2006).
[67]P. S. Weiss, P. L. Trevor, and M. J. Cardillo, Phys. Rev. B **38**, 9928 (1988).
[68]T. Klamroth and P. Saalfrank, J. Chem. Phys. **112**, 10571 (2000).
[69]D. V. Shalashilin and B. Jackson, J. Chem. Phys. **109**, 2856 (1998).
[70]S. M. Janke, M. Pavanello, G. J. Kroes, D. Auerbach, A. M. Wodtke, and A. Kandratsenka, Z. Phys. Chem. **227**, 1467 (2013).
[71]A. De Vita, I. Stich, M. J. Gillan, M. C. Payne, and L. J. Clarke, Phys. Rev. Lett. **71**, 1276 (1993).
[72]A. Groß and A. Dianat, Phys. Rev. Lett. **98**, 206107 (2007).
[73]A. Groß, ChemPhysChem **11**, 1374 (2010).
[74]P. Hohenberg and W. Kohn, Phys. Rev. **136**, B864 (1964).
[75]W. Kohn and L. J. Sham, Phys. Rev. **140**, A1133 (1965).
[76]G. Kresse and J. Hafner, Phys. Rev. B **47**, 558 (1993).
[77]G. Kresse and J. Hafner, Phys. Rev. B **49**, 14251 (1994).
[78]G. Kresse and J. Furthmüller, Comput. Mater. Sci. **6**, 15 (1996).
[79]G. Kresse and J. Furthmüller, Phys. Rev. B **54**, 11169 (1996).
[80]L. Sementa, M. Wijzenbroek, B. J. van Kolck, M. F. Somers, A. Al-Halabi, H. F. Busnengo, R. A. Olsen, G. J. Kroes, M. Rutkowski, C. Thewes, N. F. Kleimeier, and H. Zacharias, J. Chem. Phys. **138**, 044708 (2013).
[81]H. J. Monkhorst and J. D. Pack, Phys. Rev. B. **13**, 5188 (1976).
[82]K. G. Huang, D. Gibbs, D. M. Zehner, A. R. Sandy, and S. G. J. Mochrie, Phys. Rev. Lett. **65**, 3313 (1990).
[83]J. V. Barth, H. Brune, G. Ertl, and R. J. Behm, Phys. Rev. B **42**, 9307 (1990).
[84]S. Narasimhan and D. Vanderbilt, Phys. Rev. Lett. **69**, 1564 (1992).
[85]A. Groß, Phys. Rev. Lett. **103**, 246101 (2009).
[86]A. Lozano, A. Gross, and H. F. Busnengo, Phys. Chem. Chem. Phys. **11**, 5814 (2009).
[87]M. Ramos, A. E. Martínez, and H. F. Busnengo, Phys. Chem. Chem. Phys. **14**, 303 (2012).
[88]A. Groß, in *Proceedings of the NIC Symposium: 25 Years HLRZ/NIC*, edited by K. Binder, G. Münster, and M. Kremer (John van Neuman Institute for Computing, Jülich, 2012), pp. 107–114.
[89]L. Verlet, Phys. Rev. **159**, 98 (1967).
[90]L. Verlet, Phys. Rev. **165**, 201 (1968).
[91]M. Karplus, R. N. Porter, and R. D. Sharma, J. Chem. Phys. **43**, 3259 (1965).
[92]G. J. Kroes, Phys. Chem. Chem. Phys. **14**, 14966 (2012).
[93]P. M. Echenique, R. M. Nieminen, and R. H. Ritchie, Solid State Commun. **37**, 779 (1981).
[94]P. M. Echenique, R. M. Nieminen, J. C. Ashley, and R. H. Ritchie, Phys. Rev. A **33**, 897 (1986).
[95]J. I. Juaristi, A. Arnau, P. M. Echenique, C. Auth, and H. Winter, Phys. Rev. Lett. **82**, 1048 (1999).
[96]H. Winter, J. I. Juaristi, I. Nagy, A. Arnau, and P. M. Echenique, Phys. Rev. B **67**, 245401 (2003).
[97]B. Baule, Ann. Phys. (Berlin) **349**, 145 (1914).
[98]R. Cooper, I. Rahinov, C. Yuan, X. M. Yang, D. J. Auerbach, and A. M. Wodtke, J. Vac. Sci. Technol. A **27**, 907 (2009).
[99]C. T. Rettner, D. J. Auerbach, J. C. Tully, and A. W. Kleyn, J. Phys. Chem. **100**, 13021 (1996).
[100]J. C. Vickerman and I. S. Gilmore, *Surface Analysis - The Principle Techniques*, 2nd ed. (Wiley, 2009).
[101]M. S. Mizielinski, D. M. Bird, M. Persson, and S. Holloway, Surf. Sci. **602**, 2617 (2008).
[102]D. M. Bird, M. S. Mizielinski, M. Lindenblatt, and E. Pehlke, Surf. Sci. **602**, 1212 (2008).
[103]M. S. Daw and M. I. Baskes, Phys. Rev. B **29**, 6443 (1984).
[104]S. M. Foiles, M. I. Baskes, and M. S. Daw, Phys. Rev. B **33**, 7983 (1986).
[105]K. W. Jacobsen, P. Stoltze, and J. K. Nørskov, Surf. Sci. **366**, 394 (1996).
[106]J. Behler, Phys. Chem. Chem. Phys. **13**, 17930 (2011).
[107]K. V. J. Jose, N. Artrith, and J. Behler, J. Chem. Phys. **136**, 194111 (2012).

This article is copyrighted as indicated in the article. Reuse of AIP content is subject to the terms at: http://scitation.aip.org/termsconditions. Downloaded to IP: 134.76.223.157 On: Thu, 18 Sep 2014 11:16:10